VERSITA

GEOCHRONOMETRIA 41(3) 2014: 178–201
DOI 10.2478/s13386-013-0160-3

Available online at
www.springerlink.com

REVIEW AND ASSESSMENT OF THE POTENTIAL OF POST-IR IRSL DATING METHODS TO CIRCUMVENT THE PROBLEM OF ANOMALOUS FADING IN FELDSPAR LUMINESCENCE

BO LI[1], ZENOBIA JACOBS[1], RICHARD G. ROBERTS[1] and SHENG-HUA LI[2]

[1]*Centre for Archaeological Science, School of Earth and Environmental Sciences, University of Wollongong, Wollongong, NSW 2522, Australia*

[2]*Department of Earth Sciences, The University of Hong Kong, Pokfulam Road, Hong Kong, China*

Received 30 January 2013 Accepted 10 April 2014

Abstract: Quartz has been the main mineral used for optically stimulated luminescence (OSL) dating of sediments over the last decade. The quartz OSL signal, however, has been shown to saturate at relatively low doses of ~200–400 Gy, making it difficult to be used for dating beyond about 200 thousand years (ka), unless the environmental dose rate is low. The infrared stimulated luminescence (IRSL) from feldspars has been shown to continue to grow to higher dose levels than quartz OSL. The application of IRSL dating of feldspars, however, has long been hampered by the anomalous fading effect. Recent progress in understanding anomalous fading of the infrared stimulated luminescence (IRSL) signals in potassium-feldspar has led to the development of post-IR IRSL (pIRIR) protocols and also a multiple elevated temperature (MET) stimulation (MET-pIRIR) protocol. These procedures have raised the prospect of isolating a non-fading IRSL component for dating Quaternary deposits containing feldspars. In this study, we review the recent progress made on (1) overcoming anomalous fading of feldspar, and (2) the development of pIRIR dating techniques for feldspar. The potential and problems associated with these methods are discussed.

Keywords: K-feldspar, infrared stimulated luminescence, post-IR IRSL, MET-pIRIR.

1. INTRODUCTION

Quartz has been the main mineral used for optical dating of sediment over the last decade since the development of the single aliquot regenerative-dose (SAR) protocol (Galbraith *et al.*, 1999; Roberts *et al.*, 1999; Murray and Wintle, 2000). The fast component of the OSL signal in quartz has been used for dating as it is rapidly bleached (Wintle and Murray, 2006), but has been shown to saturate at relatively low doses of ~200 to 400 Gy. This has restricted its use for dating of sediments younger than about 200 thousand years (ka), unless the environmental dose rate is low (e.g., <1 Gy/ka).

Feldspars can also be used for optical dating, either using visible wavelengths for stimulation or using infrared (IR) stimulation to produce an IR stimulated luminescence (IRSL) signal (Hütt *et al.*, 1988). Compared to quartz, feldspars have several advantages in optical dating (e.g., Aitken, 1998; Huntley and Lamothe, 2001). First, the IRSL signal from feldspar usually saturates at much higher dose levels compared to quartz OSL; this is advantageous in the context of extending the dating range of optical dating for sedimentary deposits. Second, the IRSL signal is usually inherently brighter than the quartz

Corresponding author: B. Li
e-mail: bli@uow.edu.au

ISSN 1897-1695 (online), 1733-8387 (print)

OSL signal. This enables higher precision luminescence measurements to be made, generally leading to better reproducibility of the natural and laboratory-dose measurements (Li *et al.*, 2007b). Third, in the case of sand-sized grains of alkali feldspars (K-feldspars), the high contribution to the internal dose rate from ^{40}K and ^{87}Rb within the crystal lattice creates more luminescence, resulting in increased precision of the measured equivalent dose (D_e) for young samples. This higher internal dose rate also reduces the effect that inhomogeneity in the beta and gamma-dose rate spheres and water content can have on the total dose rate, resulting in improved precision. Furthermore, an isochron dating method utilising the internal dose rate of K-feldspars can also be used to overcome changes in the environmental dose rate (Li *et al.*, 2007a; Li *et al.*, 2008a; Li *et al.*, 2008b). Despite all these advantages, feldspars have long been known to exhibit a phenomenon called anomalous fading (Wintle, 1973; Spooner, 1992, 1994; Huntley and Lamothe, 2001; Huntley and Lian, 2006). Anomalous fading relates to the leakage of electrons from traps that give rise to IRSL at a much faster rate than would be expected from kinetic considerations. This phenomenon has hampered the application of luminescence dating of feldspar extracted from sediment for many years.

Recent progress in understanding anomalous fading of feldspar has raised the prospect of isolating a non-fading IRSL component for dating Quaternary deposits containing feldspars. By first bleaching feldspar grains using IR photons at 50°C and then measuring the post-IR IRSL (pIRIR) signal at an elevated temperature (>200°C), it is possible to preferentially sample the electrons from the traps that suffer least from fading (Thomsen *et al.*, 2008). Since the initial observation, different pIRIR procedures have been developed, including a two-step (e.g., Thomsen *et al.*, 2008; Buylaert *et al.*, 2009; Thiel *et al.*, 2011a) and a multiple elevated temperature (MET) post-IR IR stimulation procedure (Li and Li, 2011a; 2012a).

In this paper, we summarise the results from over 300 samples presented in recently published studies using different pIRIR signals (**Table S1**). We focused on various luminescence behaviours and the performance of the SAR procedure when measuring the pIRIR signals, and we also discuss the potential and problems of using the pIRIR signals for dating sediments.

2. ANOMALOUS FADING

Anomalous fading was first observed for volcanic feldspars measuring their thermoluminescence (TL) signals (Wintle, 1973). It was subsequently also reported for IRSL signals from a wide range of feldspars extracted from sediments (Spooner, 1994; Huntley and Lamothe, 2001; Huntley and Lian, 2006). Anomalous fading has been suggested to be the main reason for underestimation of D_e when IRSL measurements are made shortly after irradiation (Spooner, 1994; Huntley and Lamothe, 2001).

Anomalous fading in feldspars has been explained as a result of tunnelling recombination between electron-hole pairs (e.g., Aitken, 1985; Visocekas, 1985; Visocekas *et al.*, 1994). This explanation is strongly supported by the observation of phosphorescence when recently irradiated samples were cooled down to liquid nitrogen temperatures (Visocekas, 1985). The extent of anomalous fading can be quantified using a laboratory fading test, which involves measuring the signal decay after irradiation and different delay periods (Huntley and Lamothe, 2001; Auclair *et al.*, 2003). Decay of the IRSL signal as a function of storage time appears to follow a power law with linear decay on a log (time) scale, which enables the calculation of a fading rate (g-value) expressed as percentage loss per decade, where a decade is a factor of 10 in time since laboratory irradiation (Aitken, 1985). Huntley and Lamothe (2001) demonstrated that anomalous fading was ubiquitous across Canada regardless of geological origin and this was later confirmed by Huntley and Lian (2006) who measured g-values of 3–7% per decade for most of the 77 samples of K-feldspar that they extracted from sediments around the world. These findings suggested that anomalous fading is a universal phenomenon for feldspars.

Given the great potential for extending the age range of luminescence dating using feldspar, a number of attempts have been made over the last two decades or so to avoid anomalous fading (e.g., Sanderson and Clark, 1994; Lamothe and Auclair, 1999; Huntley and Lamothe, 2001; Zhao and Li, 2002; Lamothe *et al.*, 2003; Tsukamoto *et al.*, 2006; Li *et al.*, 2008b). One such attempt was the storage of mineral grains such as zircon at elevated temperatures before measurement of the TL signal, which Templer (1985) found removed anomalous fading. Spooner (1992), however, later reported that the fading for a labradorite was unchanged regardless of whether the sample was stored at 10 or 100°C. Another method proposed by Sanderson and Clark (1994) used time-resolved signals. They suggested that different parts of the pulsed OSL signal of feldspar have different fading rates, and anomalous fading might be avoided by selecting those parts of the signal that do not fade. A similar conclusion was reached by Tsukamoto *et al.* (2006) and Jain and Ankjærgaard (2011). In a later study, Li *et al.* (2008b) proposed an isochron IRSL dating method, which uses the IRSL signal from K-feldspar grains of different grain sizes. This method appears to avoid the problem of anomalous fading (Li *et al.*, 2007a; Li *et al.*, 2008a; Li *et al.*, 2008b). They suggested that the internal dose is responsible for generating a non-fading signal, but the underlying mechanism remains controversial (Huntley, 2011; Li *et al.*, 2011) and the application of this method is restricted to aeolian samples with homogeneous grain-to-grain luminescence characteristics.

Several methods have also been developed to correct for anomalous fading. Lamothe and Auclair (1999) proposed 'the fadia method' using single-grain IRSL measurements. This involves calculation of a ratio ($R_I(t)$) of the luminescence measured after a laboratory irradiation compared to that measured before irradiation (Lamothe and Auclair, 1997). By comparing the values R_I measured at different delay times ($R_I(t_1)$ and $R_I(t_2)$), a value of R_I representing no fading can be obtained by extrapolation. This R_I value is then used to correct the growth curve to obtain a corrected age. Huntley and Lamothe (2001) also proposed a method to correct for anomalous fading, based on the measurement of the g-value. This correction method was later simplified by Lamothe *et al.* (2003) by incorporating the environmental and laboratory dose rates into the equation. A major drawback of these correction methods are that their application is restricted to relatively young sediments (e.g., younger than ~20–50 ka or 100 ka in low dose rate environments) with linear dose-response curves. For older samples, such methods also become unreliable due to the dependency of the anomalous fading rate on the size of the natural dose received (Kars *et al.*, 2008; Li and Li, 2008; Morthekai *et al.*, 2008). It would thus appear that most of these methods are more or less model- or sample-dependent, which limits standard application of feldspar IRSL dating similar to what we have become accustomed to for quartz OSL dating. Targeting a non-fading signal, therefore, appears to be the best way forward so that anomalous fading can be avoided all together.

3. IDENTIFICATION OF A NON-FADING SIGNAL

Two-step post-IR IRSL

Although Wintle (1973) reported anomalous fading of thermoluminescence (TL) in feldspars, Valladas and Valladas (1979) and other subsequent studies (e.g., Guérin and Valladas, 1980) found that the high temperature TL of plagioclase feldspars is not affected by fading. Jain and Singhvi (2001) made similar observations for the optical signal when they observed that IR bleaching of feldspars at 220°C resulted in a remnant population of more thermally stable traps that could potentially be probed by high temperature IR stimulation. Following this suggestion, Thomsen *et al.* (2008) found that IR signals stimulated at 225°C faded much less than those stimulated at 50°C and that the later part of the IRSL signal exhibits a lower fading rate compared to its initial part. They suggested that the IRSL signal observed at a low stimulation temperature (e.g., 50°C) is mainly the result of tunnelling between spatially close donor-acceptor pairs, while the signal observed at higher stimulation temperatures is the result of tunnelling between spatially distant donor-acceptor pairs or thermally-assisted hopping among band-tail states. Since anomalous fading is a result of tunnelling between spatially close donor-acceptor pairs, they expected that prolonged exposure to IR at a low stimulation temperature should deplete the spatially close (or easy-to-fade) donor-acceptor pairs and lead to a reduction in the fading component. This led to the development of a two-step post-IR IRSL dating method (Thomsen *et al.*, 2008) in which an IR stimulation at a lower temperature (T1) is applied before measurement of the IRSL signal at a higher temperature (T2) (**Table 1**). Since then, different versions of the pIRIR method, using different combinations of IR stimulation temperatures (T1 and T2), have been proposed. Here we will use the term 'pIRIR(T1, T2)' to refer to the temperatures used in the different two-step pIRIR procedures.

Thomsen *et al.* (2008) first tested the anomalous fading rate of the pIRIR signal measured at 225°C after an initial IRSL measurement at 50°C (pIRIR(50, 225)) and a preheat of 250°C for 60 s. They found that the laboratory

Table 1. *The two-step pIRIR and multi-elevated-temperature pIRIR (MET-pIRIR) protocols.*

Post-IR IRSL protocols		
Step	**Treatment**	**Observed**
	Two-step pIRIR protocol	
1	Give regenerative dose, D_i[a]	
2	Preheat at 250 or 320°C for 60 s[b]	
3	IRSL measurement at T1 for 200 s	$L_{x(50)}$
4	IRSL measurement at T2 for 200 s	$L_{x(T)}$
5	Give test dose, D_t	
6	Preheat at 250 or 320°C for 60 s[b]	
7	IRSL measurement at T1 for 200 s	$T_{x(50)}$
8	IRSL measurement at T2 for 200 s	$T_{x(T)}$
9	IR bleaching at 325°C for 40 s	
10	Return to step 1	
	MET-pIRIR protocol	
1	Give regenerative dose, D_i[a]	
2	Preheat at 320°C for 60 s	
3	IRSL measurement at 50°C for 100 s	$L_{x(50)}$
4	IRSL measurement at 100°C for 100 s	$L_{x(100)}$
5	IRSL measurement at 150°C for 100 s	$L_{x(150)}$
6	IRSL measurement at 200°C for 100 s	$L_{x(200)}$
7	IRSL measurement at 250°C for 100 s	$L_{x(250)}$
8	IRSL measurement at 300°C for 100 s	$L_{x(300)}$
9	Give test dose, D_t	
10	Preheat at 320°C for 60 s	
11	IRSL measurement at 50°C for 100 s	$T_{x(50)}$
12	IRSL measurement at 100°C for 100 s	$T_{x(100)}$
13	IRSL measurement at 150°C for 100 s	$T_{x(150)}$
14	IRSL measurement at 200°C for 100 s	$T_{x(200)}$
15	IRSL measurement at 250°C for 100 s	$T_{x(250)}$
16	IRSL measurement at 300°C for 100 s	$T_{x(300)}$
17	IR bleaching at 325°C for 100 s	
18	Return to step 1	

[a] For the 'natural' and sunlight-bleached samples, i = 0 and D_0 = 0. The whole sequence is repeated several times using a series of different regenerative doses including a zero dose and a repeat dose.

[b] For the pIRIR(50, 225) method (Buylaert et al., 2009), the preheat temperature is 250°C. For the pIRIR(50, 290) method (Thiel et al., 2011a), the preheat temperature is 320°C.

fading rate of the pIRIR(50, 225) signal is significantly lower than for the corresponding 50°C IRSL signal, and the magnitude of the fading correction largely reduced. Similar observations were reported in subsequent studies (e.g., Buylaert *et al.*, 2009; Alappat *et al.*, 2010; Lowick *et al.*, 2012; Sohbati *et al.*, 2012; Vasiliniuc *et al.*, 2012). In **Fig. 1a** and **1b**, we have compared the g-values calculated for the 50°C IRSL and pIRIR(50, 225) signals provided in previously published studies (see **Table S1** for values and references). The frequency histograms of the same data sets are also shown in **Fig. 1c**. It shows large sample-to-sample variation in g-values obtained for the 50°C IRSL signal (from ~1 to ~15 %/decade). This contrasts with the results obtained for the pIRIR(50, 225) signal for which all, but two, of the samples had g-values that fall within a narrow range of ~0.5 to ~3%/decade. In addition, the pIRIR(50, 225) g-values are also systematically smaller than those observed for the 50°C IRSL signal (**Fig. 1a** and **1b**) with average fading rates of 3.7 ± 0.3 and 1.5 ± 0.1 %/decade for the 50°C IRSL and pIRIR(50, 225) signals, respectively. If we were to use these two g-values to correct the age of a sample with an apparent age of 50 ka, using the method of Huntley and Lamothe (2001) and assuming that both the g-values and D_e values were normalised to a delay time (t_c) of 2 days, the percentage age correction would be ~32 and ~11%, respectively. The uncertainty on the age associated with the fading correction for the pIRIR(50, 225) signal is, therefore, significantly reduced compared to the age correction for the 50°C IRSL, as previously shown by Buylaert *et al.* (2009).

Following the initial work of Thomsen *et al.* (2008) and Buylaert *et al.* (2009), Thiel *et al.* (2011a) proposed a modified method to measure the pIRIR signal following a higher preheat temperature (320°C compared to 250°C) and IR stimulation at a higher temperature (T2 = 290°C compared to 225°C) (*i.e.*, pIRIR(50, 290)). This method (pIRIR(50, 290)) was subsequently tested in thirteen

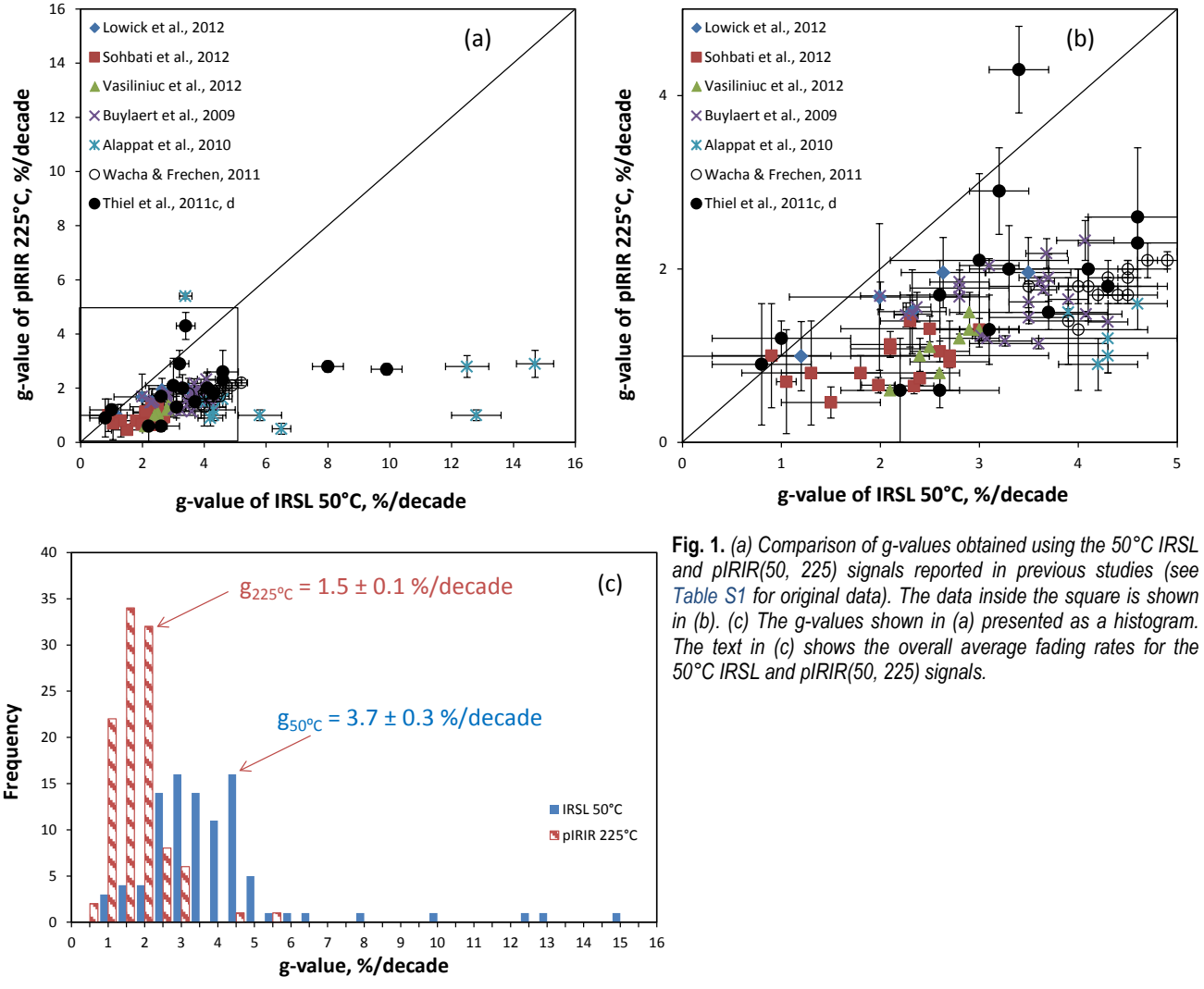

Fig. 1. *(a) Comparison of g-values obtained using the 50°C IRSL and pIRIR(50, 225) signals reported in previous studies (see Table S1 for original data). The data inside the square is shown in (b). (c) The g-values shown in (a) presented as a histogram. The text in (c) shows the overall average fading rates for the 50°C IRSL and pIRIR(50, 225) signals.*

different studies (see summary in **Table S1** and reference therein). All measured g-values reported in the 13 studies are provided in **Table S1** and those g-values calculated for the pIRIR(50, 290) signal are summarised in **Fig. 2** and compared to those obtained for the pIRIR(50, 225) signal. Note that the g-values for the two signals shown in **Fig. 2** are not all on the same set of samples. A range of g-values between ~0 and ~5 %/decade was observed for different samples from different regions of the world, and most of the values fall between ~0.5 and ~2%/decade. An average value of 1.1 ± 0.1 %/decade is calculated for the pIRIR(50, 290) signal, and this is smaller than the average value of 1.5 ± 0.1 %/decade obtained for the pIRIR(50, 225) signal.

There are 37 samples from 6 different studies for which g-values and ages were calculated using both pIRIR(50, 225) and pIRIR(50, 290) (Buylaert *et al.*, 2009, 2011, 2012; Thiel *et al.*, 2011c; Lowick *et al.*, 2012; Vasiliniuc *et al.*, 2012); the g-values are compared in **Fig. 3a**. This data set represents samples from a range of geographic regions and different depositional environments, including loess, aeolian, coastal and waterlain sediments. Sixy-five percent of the samples (n = 24) have g-values for both signals that are statistically consistent with each other at 2σ and range between 2.0 ± 0.4 and 0.6 ± 0.2%/decade for the pIRIR(50, 225) signal and between 3.7 ± 1.3 and 0.6 ± 0.1%/decade for the pIRIR(50, 290) signal. The remaining 35% of the samples (n = 13) have g-value for the pIRIR(50, 290) signal (g290-value) that are all smaller than the corresponding g-values for the pIRIR(50, 225) signal (g225-value); the g225values range between 2.9 ± 0.5 and 1.2 ± 0.03 %/decade and the g290-values range between 1.53 ± 0.05 and –0.4 ± 0.05 %/decade. Where there is consistency, the g225-values are on average larger than those that show no consistency with their corresponding g290-values at 2σ (**Fig. 3a**).

Fig. 3b shows the fading-uncorrected ages for the same set of samples for which fading rates are provided in **Fig. 3a**; note that 5 of the 37 samples are not shown as their ages are only reported as minimum ages without error estimates (see **Table S1**). The different symbols differentiate between those samples that have consistent g-values at 2σ (g225 = g290; circles), and those that have g225-values that are larger than their corresponding g290-values (g225 > g290; squares). **Fig. 3b** shows good agreement between ages obtained from both methods for samples <100 ka (see inset plot). This is consistent with the g-values that are either consistent or relatively small (<~2%/decade). For those samples >100 ka it appears that the pIRIR290 age on average overestimate relative to their corresponding pIRIR225 ages, shown by the majority of samples falling above the 1:1 line (solid line). We have also fitted a weighted linear fit to all the samples >20 ka presented in **Fig. 3b** (indicated as a broken line); the slope of the line is 1.20 ± 0.03 and the interception is 1.9 ± 1.5 ka on the y-axis. We omitted the <20 ka samples as these may be affected by the presence of a relatively large residual dose (see below). This pattern does not change if we omit the two oldest ages that were reported to be in, or close to, saturation (Vasiliniuc *et al.*, 2012). Since the pIRIR290 signal is more likely to be incompletely bleached than the pIRIR225 signal, it is important to ensure that the samples were well-bleached at the time of deposition. Among the samples presented in **Fig. 3b**, most of them are aeolian sediments, which are expected to have been well-bleached. Exceptions are two waterlain samples (GOS3 and ZEL7) from Switzerland (Lowick *et al.*, 2012), which may have been incompletely bleached, although one of them (GOS3) was considered well-bleached by the authors, based on the fact that the ages obtained from a variety of luminescence signals were in agreement with uranium-series and radiocarbon ages (Lowick *et al.*, 2012). If we discard these two samples from our analysis, however, the pattern shown in **Fig. 3b** does not change. Thus we consider that the overestimation in pIRIR290 ages relative to pIRIR225 ages shown in **Fig. 3b** is not due to the problem of insufficient bleaching.

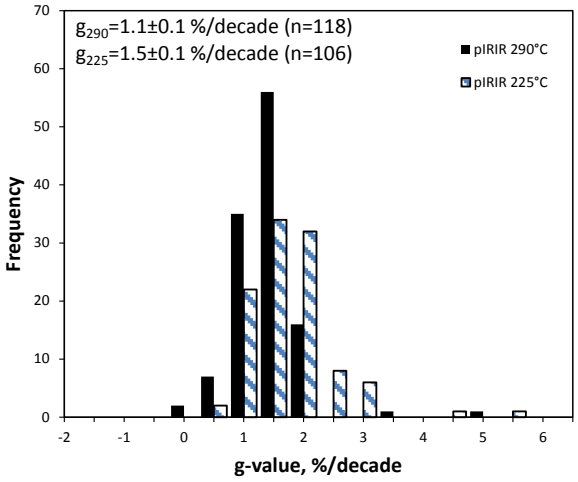

Fig. 2. *A summary of the g-values measured using pIRIR(50, 290) and those using pIRIR(50, 225) signals in previous studies (see Table S1 for original data).The text in the figure shows the average fading rates for the two signals.*

To further scrutinise the results, we have plotted the same data in **Fig. 3c** but this time as age ratios (pIRIR290 / pIRIR225) plotted from youngest on the left to oldest on the right using their pIRIR(50, 290) ages for ranking. From here it can be seen that 2 of the 5 samples (40%) younger than ~20 ka, 7 of the 9 samples (78%) between ~20 and 100 ka, and 9 of the 18 samples (50%) older than 100 ka have fading-uncorrected ages consistent with each other at 2σ. The difference in age is, therefore, most conspicuous not only for those samples older than ~100 ka, but also for young samples (<20 ka). Importantly, there is no direct relationship between consistency in fading rate

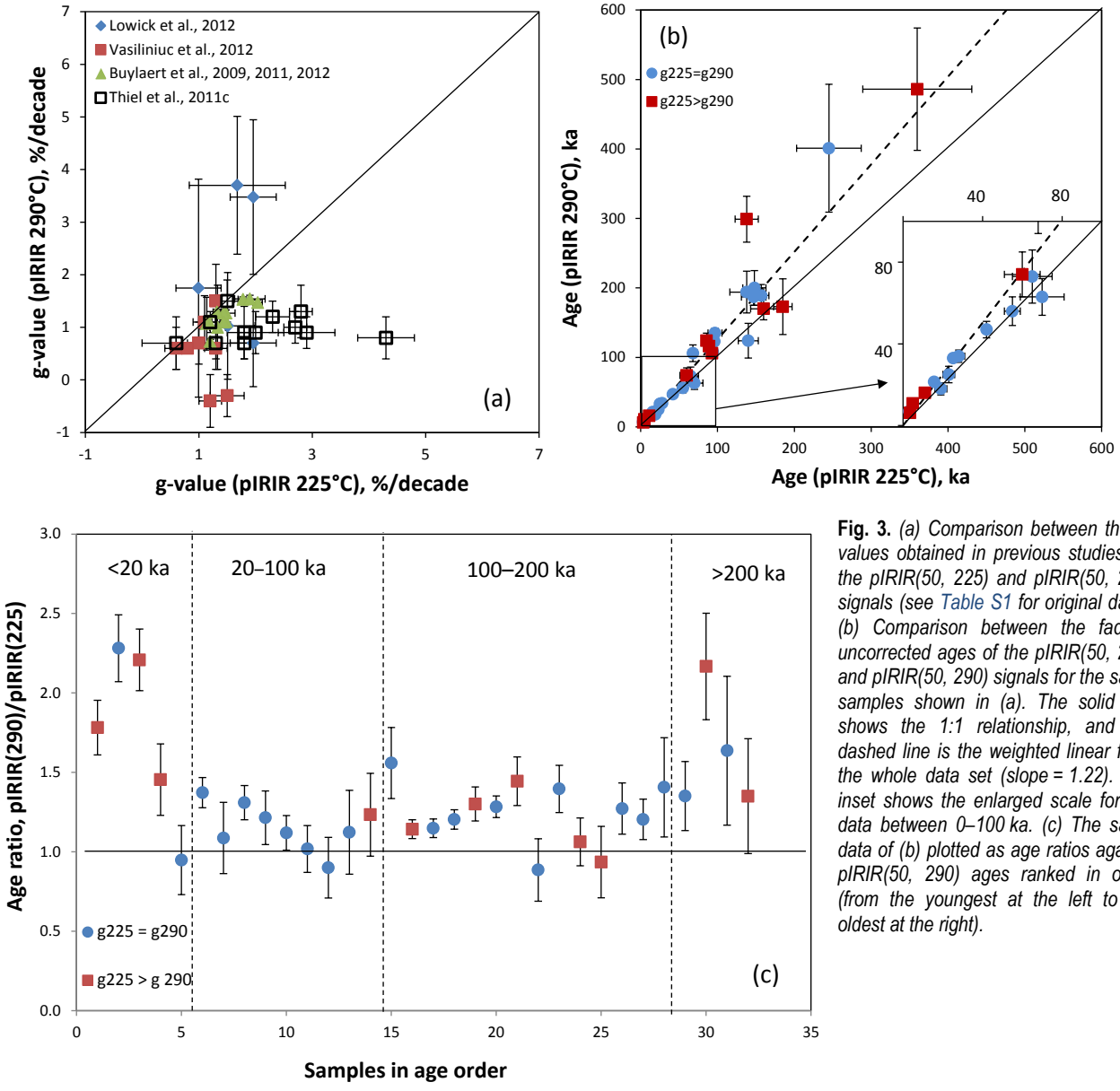

Fig. 3. *(a) Comparison between the g-values obtained in previous studies for the pIRIR(50, 225) and pIRIR(50, 290) signals (see Table S1 for original data). (b) Comparison between the fading-uncorrected ages of the pIRIR(50, 225) and pIRIR(50, 290) signals for the same samples shown in (a). The solid line shows the 1:1 relationship, and the dashed line is the weighted linear fit of the whole data set (slope = 1.22). The inset shows the enlarged scale for the data between 0–100 ka. (c) The same data of (b) plotted as age ratios against pIRIR(50, 290) ages ranked in order (from the youngest at the left to the oldest at the right).*

and age; samples with g225 = g290 value can have consistent and inconsistent ages between the two signals and the same is true for samples with g225 > g290 values. A weighted mean ratio (pIRIR290/pIRIR225) of 1.21 ± 0.05 for the ages of samples older than 20 ka suggests that the pIRIR(50, 290) ages are on average older than their respective pIRIR(50, 225) ages by ~20%. The weighted mean ratio for the samples between 20 and 100 ka is 1.19 ± 0.05 and for those >100 ka the ratio is 1.22 ± 0.07; the latter ratio changes to 1.21 ± 0.07 if the two oldest samples are omitted. So, even though there appear to be a systematic trend with age, the differences are similar on average regardless of age.

Several possible reasons may explain the systematic overestimation in age for the pIRIR(50, 290) signal compared to the pIRIR(50, 225) signal. 1) The first explanation is that a small difference in fading rate between the two pIRIR signals could result in a large difference in apparent age. We can use the >20 ka samples shown in **Fig. 3** as a point in case. For these samples the pIRIR(50, 290) ages are on average ~20–30% older than their corresponding pIRIR(50, 225) ages (**Fig. 3b**). The average g-value for the pIRIR(50, 225) signal is 1.5%/decade and for the pIRIR(50, 290) signal, 1.1%/decade. If the true age of the samples is 50 ka and we use these average g-values to calculated apparent ages, using the equation of Huntley and Lamothe (2001), then apparent ages of ~45 and ~46 ka are obtained. Note that this difference will become larger for older samples where the fading correction method is not applicable. The difference in age,

however, will still be too large to be explained by differences in the g-values, and the difference in age can, therefore, not be explained by the difference predicted by the laboratory-measured fading rates.

A second explanation, first proposed by Thiel *et al.* (2011a), is that the fading rates measured in the laboratory for the pIRIR(50, 290) signal are artefacts (*i.e.*, they are not real). They found support in this from natural pIRIR(50, 290) signals measured for infinitely old samples that are close to or in dose saturation, compared to natural pIRIR(50, 225) signals for the same samples that are consistently found to be ~15–20% below saturation. So, following this argument, a number of recent studies have proposed that the pIRIR(50, 290) signal is stable and does not fade, and that the difference in age between the two pIRIR signals are due to the fading of one, but not the other (Thiel *et al.*, 2011a; Stevens *et al.*, 2011; Buylaert *et al.*, 2012). If this is the case, then there will also be systematic errors associated with the dose response curves (DRC) and the estimated D_e values because the same SAR procedure is used for estimation of the fading rate and construction of DRCs. The extent of the introduced error on the different measurements and components will, however, be significantly different and should be assessed separately (*i.e.*, a small change in the g-value can significantly change the age, whereas a small change in the DRC or D_e may not be so important). One would, however, expect the recycling ratio for the pIRIR(50, 290) signal to deviate systematically from unity if the fading rate is an apparent result of a systematic decrease of the repeated measurement of the regenerative-dose signals in the SAR cycles in the fading test. This is, however, not supported by the result of a large number of recycling ratios that are consistent with unity (see Fig. 3A in Buylaert *et al.* (2012)). What also remains unclear is why the one signal (pIRIR(50, 225)) would fade and not the other (pIRIR(50, 290)). The measurement conditions of the two signals are different in terms of preheat temperature (250°C for pIRIR(50, 225) and 320°C for pIRIR(50, 290)) and the pIRIR stimulation temperature (225 and 290°C). Both signals are measured after the prolonged 50°C IRSL stimulation that is used to deplete the 'easy-to-fade' donor-acceptor pairs. If this stimulation did not remove the entire fading component, then the remainder should presumably be sampled by the subsequent pIRIR measurement, regardless of whether it is measured at 225°C or 290°C. The higher preheat temperature used for pIRIR(50, 290) could also remove more easy-to-fade electron-hole pairs and, therefore, leave more difficult-to-fade components in the subsequent IRSL signals (e.g., Jain and Ankjærgaard, 2011). This high preheat temperature, however, does not eliminate the fading component completely, because the subsequent IRSL 50°C signal still yields a large fading rate (**Fig. 1b**). It is reasonable to deduce, therefore, that the lower fading rate observed in pIRIR(50, 290) signal is due mainly to the higher stimulation temperature used, although a higher preheat temperature may still play a role. Following this logic, either both signals should fade (although may be to different extents), or both signals do not fade and the measured fading rates are laboratory artefacts. If both measured fading rates are artefacts, then both signals should give similar ages; this is true for some, but not all of the samples shown in **Fig. 3b** and **3c**.

A third possible explanation was proposed by Vasiliniuc *et al.* (2012) and Chen *et al.* (2013) who suggested that the D_e obtained using the pIRIR(50, 290) signal is overestimated in some samples because of an unsuccessful sensitivity correction of the first measurement (*i.e.*, the natural signal). Fading rate measurements do not involve measurement of the natural signal either in D_e or dose recovery measurements, so the problem of the sensitivity correction of the natural is avoided. If this explanation is true, then the pIRIR(50, 290) ages for old samples (e.g., >100 ka) should be treated with caution because any slight error in the sensitivity correction will result in a relatively large uncertainty in the large dose range of DRCs. This possibility can, however, be tested by conducting a dose recovery test (see section 4). Apart from the problem of natural sensitivity correction, the presence of an isothermal signal (Fu *et al.*, 2012a; Wang and Wintle, 2013) was also proposed to be a potential problem for measurement of the natural dose and overestimation of the age. We note that any pIRIR signal can contain some thermal signal, especially when the difference between the preheat and pIRIR stimulation temperatures is small (*i.e.*, 25 and 30°C for pIRIR(50, 225) and pIRIR(50, 290) signals, respectively). However, the effect of the isothermal signal on D_e estimation may differ between the two pIRIR signals, due to the large difference in thermal stability of the 225 and 290°C signals. In both cases, one should monitor for and wait long enough to reduce the thermal signal before starting IR stimulation (Fu *et al.*, 2012a).

Multi-step post-IR IRSL

Li and Li (2011a) proposed a multi-step pIRIR procedure (**Table 1**), the so-called multi-elevated-temperature post-IR IRSL (MET-pIRIR) protocol as an alternative to the two-step procedures. This method is based on the observation that the fading component in the IRSL signal can be progressively eliminated using multiple IR stimulations by increasing the stimulation temperature from 50 to 250°C in 50°C intervals. Laboratory fading tests for a feldspar sample showed that the highest anomalous fading rate is observed for the 50°C IRSL, and it decreases as the stimulation temperature is increased. Negligible anomalous fading rates were observed for the signals obtained at 250°C (**Fig. S2**) (Li and Li, 2011a; 2012a).

One advantage of the MET-pIRIR protocol over the two-step pIRIR protocol is that the effect of anomalous fading can be demonstrated in an Age_Temperature (A-T) or a D_e_Temperature (D_e-T) plot, in which the calculated ages or D_e are plotted as a function of IR

stimulation temperature (**Fig. 4**). The A-T (or D_e-T) plot shows how the ages increase with increased stimulation temperature until an age plateau (shown as a broken line in **Fig. 4**) is reached at higher temperatures; this plateau indicates that a non-fading component was isolated at elevated temperatures. The age plateau could, therefore, be used as a internal diagnostic tool for checking whether a stable, non-fading component has been achieved or not. The MET-pIRIR protocol was first tested using various sedimentary samples from northern China deposited over the last ~130 ka (Li and Li, 2011a). For all of the samples, the youngest ages were obtained using 50°C IRSL from where ages obtained for subsequently measured MET-pIRIR signals started to increase as a function of an increase in stimulation temperature until an age or D_e plateau is obtained above 200°C. This method was subsequently tested on loess samples from the Luochuan section of the Chinese Loess Plateau (Li and Li, 2012a). In **Fig. 4**, we compiled a summary A-T or D_e-T plot containing data of 46 samples from Northern China, India and Europe (see **Table S1** for samples, D_e values and ages). To facilitate comparisons, all ages or D_e values were first normalised to 1 at 250°C. The samples were divided into four groups according to their age (*i.e.*, <50, 50–100, 150–200 and >200 ka) and the average values of the samples from each group was calculated and shown in **Fig. 4**. The error on each average value is the 1σ standard deviation. It is observed that the temperature at which the plateau is reached varies with age. Younger samples (<50 ka), appear to reach the plateau at ~200°C, whereas older samples (50–200 ka) only reach the plateau at ~250°C. The data set for the oldest samples (>200 ka), however, appears to be keep increasing with stimulation temperature — that is, the normalised D_e value at 300°C is 1.1 ± 0.1 for these samples. Note that the latter value is based on 3 samples only, because most of the samples have saturated MET-pIRIR 300°C signals; the signals obtained at lower temperatures were not saturated for the 9 samples investigated. The results of **Fig. 4** indicate that the MET-pIRIR 200°C signal (and probably the 250°C signal also) still suffers from a small amount of fading, which has a negligible effect on young samples (e.g., <50 ka), but that manifest itself in a more significant underestimation of age or D_e in older samples. Fu and Li (2013) also reported that an age plateau, consistent with the expected age for their Holocene-age samples, can be achieved at temperatures as low as ~150°C. Another important feature of **Fig. 4** is that older samples tend to show a larger difference in age or D_e between low-temperature IRSL and high-temperature MET-pIRIR, suggesting that older samples have a higher effective anomalous fading rate associated with the low-temperature IRSL signal (Li and Li, 2008).

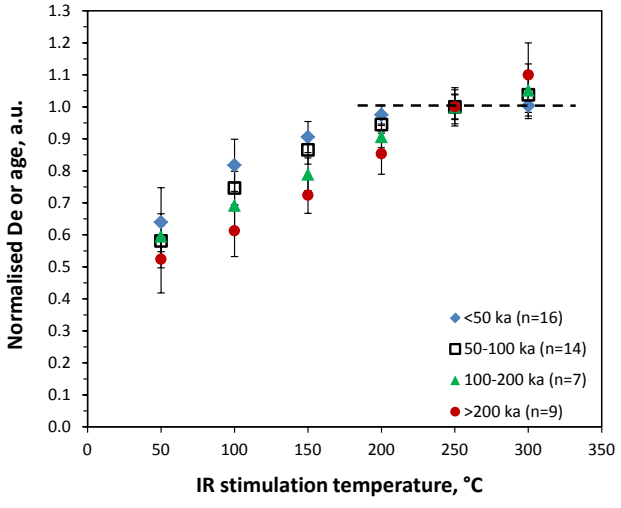

Fig. 4. *Normalised ages (or D_e) plotted against IR stimulation temperature for different samples in different age ranges (<50, 50–100, 100–200 and >200 ka). The MET-pIRIR ages were normalised to unity at 250°C, and then averaged for each group. The dashed horizontal line shows the normalised value at 1. The number of samples (n) used to produce the data set is shown in the legend. Note that the data point at 300°C for the data set of >200 ka is based on 3 samples only because most of the samples have saturated MET-pIRIR 300°C signals, although the signals obtained at lower temperatures were not saturated for the 9 samples investigated.*

Another advantage of the A-T plot is that it can be used as an indicator of insufficiently bleached samples. An insufficiently bleached sample is unlikely to give an age plateau when plotted as an A-T plot, because the MET-pIRIR signals obtained at higher temperatures are more difficult to bleach than the low temperature signals (Li and Li, 2011a). When using the A-T plot to diagnose the problem of insufficient bleaching, two factors — bleaching and fading — must be considered. Both can influence the pattern of the plateau, and this may cause difficulty in distinguishing partial bleaching from fading. As indicated by **Fig. 4**, however, such difficulties can mostly affect older samples (e.g., >200 ka), as even a small anomalous fading could significantly affect the ages. For younger samples, assessing incomplete bleaching is usually more important and fading can be compensated for more effectively by making a laboratory fading test; the A-T plot can then be used to diagnose the existence or absence of insufficient bleaching.

The MET-pIRIR method was subsequently tested by Thomsen *et al.* (2012) who measured 9 samples using both the MET-pIRIR and the pIRIR(50, 290) protocols. They suggested that no significant difference was observed between the results obtained from both methods for their samples, indicating that the prior-IR stimulation temperature may not be important and a single IR stimulation at 50°C may be sufficient to remove the fading component. The two methods were also tested by Li and Li (2012b) using loess samples from the Chinese Loess Plateau. They found that the pIRIR(50, 290) give comparable results for those samples with relatively small natural doses (e.g., <500 Gy), which is consistent with the findings reported by Thomsen *et al.* (2012). But, the

pIRIR(50, 290) signal starts to underestimate relative to the MET-pIRIR ages for older samples with larger natural doses (>500 Gy), suggesting that a small fading component may still be present in the pIRIR(50, 290) signal and, although it is not a problem for young samples, it becomes more important for older samples.

The validity of the MET-pIRIR method has so far only been tested on a small number of samples from China where independent age control is available, and its general applicability to samples from different geographical locations and depositional environments are currently been tested.

4. BEHAVIOUR OF THE POST-IR IRSL SIGNALS

Thermal stability

One of the crucial assumptions in OSL dating is that the trapped electrons used for dating are stable over the time of burial. It is thus important to ensure that the luminescence signals used for dating are associated with stable traps that have a long lifetime at ambient temperature (e.g., ~10–20°C). There have been several studies of the thermal stability of the IRSL signal for K-feldspar grains extracted from sediments (Spooner, 1994; Li and Tso, 1997; Li *et al.*, 1997; Murray *et al.*, 2009; Baril and Huntley, 2003). Focusing on the initial part of the IRSL signal obtained by stimulating at ~50°C, Li *et al.* (1997) suggested that the IRSL traps are associated with deep traps with a thermal depth of ~1.7 eV (Li *et al.*, 1997), which have a lifetime of ~10^9 years. A similar result was obtained by Murray *et al.* (2009). Based on the reduction of TL from IR bleaching, they suggested that the IRSL traps of their K-feldspar sample mainly originated from deep traps associated with the ~410°C TL peak. In a later study on the effect of IR bleaching on the TL of K-feldspar from sediments from North China, Li and Li (2011b) found that the IRSL are associated with the 350 and 400°C TL peaks, which led them to suggest that at least two groups of traps (shallow and deep) are associated with the IRSL signals. All these studies suggest that the IRSL signal from K-feldspar is thermally stable over the datable period (e.g., <1 Ma). However, based on isothermal studies of IRSL and pIRIR signals, Li and Li (2013) suggested that, although originated from deep traps, a part of the IRSL signal is still thermally unstable due to the presence of the band-tail states (Poolton *et al.*, 2002; Poolton *et al.*, 2009). They suggested that a preheat temperature above 200°C is necessary to remove these unstable signals.

The thermal stability of the pIRIR signal was investigated in several studies (Li and Li, 2011b; Thomsen *et al.*, 2011; Fu *et al.*, 2012b; Li and Li, 2013). Based on a pulse anneal study of the IRSL and pIRIR signals on the K-feldspar grains from several sedimentary samples, Thomsen *et al.* (2011) showed that the pIRIR signal has a greater thermal stability than the 50°C IRSL signal (e.g., heating to ~400°C can erase most of the 50°C IRSL signal, whereas the pIRIR(50,290) signal is still not completely erased by heating to ~550°C). Li and Li (2011b) studied the thermal stability of the IRSL and MET-pIRIR signals from K-feldspar grains. Based on their pulse anneal studies, they suggested that the MET-pIRIR signals at elevated temperatures (>100°C) are more thermally stable than the IRSL signal at 50°C, due to the presence of deeper traps in the MET-pIRIR signals. It has, however, been suggested that the difference in thermal stabilities can be explained using a single-trap model. Based on a time-resolved stimulation study, Jain and Ankjærgaard (2011) suggested that the low temperature IRSL signal and the pIRIR signal have different recombination routes; the former are dominated by recombination of spatially close electron-hole pairs and the latter are dominated by recombination of distant electron-hole pairs. They, therefore, argued that the observed difference in the thermal stabilities of IRSL and pIRIR signals can be explained as a single-trap model with the presence of band-tail states. Andersen *et al.* (2012) produced direct spectroscopic evidence that also favours a single-trap model. It is, however, difficult to explain, with a single-trap model, the different dose response curve shapes obtained from measurement of different IRSL and pIRIR signals (see section 4), and their different bleaching rates under high-energy stimulation (e.g., sunlight bleaching) (see section 4). Andersen *et al.* (2012), however, suggested that the differences in DRC shapes may be kinetic rather than a multiple trap effect. The debate about whether it is a single- or multiple-trap model is still ongoing and more data will no doubt be provided in future studies in support of one or the other of these models.

Bleachability and residuals

Another crucial precondition for luminescence dating of sediment is that the signals measured in the laboratory should be bleachable by sunlight. Although the pIRIR signals measured at elevated temperature have significantly reduced rates of fading compared to the IRSL signal measured at low temperatures (**Fig. 1c**), they have also been found to be more difficult to bleach (Thomsen *et al.*, 2008; Li and Li, 2011a). **Fig. S1** shows the solar bleaching experiments for IRSL and pIRIR signals reported by Buylaert *et al.* (2012) and Li and Li (2011a). Both studies showed that, at higher stimulation temperatures, the IRSL signal consists of components that are more resistant to sunlight bleaching, and it requires up to several hours of exposure to simulated sunlight in a solar simulator to empty most of the light-sensitive pIRIR traps. The relatively harder-to-bleach nature of the pIRIR signals, compared to the fast bleaching rate in quartz OSL, can be used to identify well-bleached quartz grains (Murray *et al.*, 2012), or can be used to identify poorly bleached feldspar grains.

A feature of the pIRIR signals, however, is that there is a non-bleachable (or residual) component left even

after a prolonged bleaching period. This manifests itself as a 'residual dose' when modern and sun-bleached sediments are measured. Apart from the 'non-bleachable' component, the residual doses observed in the pIRIR signals may also be partly induced by thermal transfer of charge from unstable light-insensitive traps into the IRSL and pIRIR traps due to the high preheat temperature (>300°C) used in the pIRIR protocols (Buylaert *et al.*, 2012). No matter which source the residual dose is from, it needs to be taken into consideration for D_e estimation.

In previous studies, estimates of the size of the residual dose have been made from measurements of modern analogues or samples of interest that have been artificially bleached with a solar simulator or natural sunlight. A small residual dose up to a few Gy in the pIRIR signal has been reported (e.g., Thomsen *et al.*, 2008; Li and Li, 2011a; Fu *et al.*, 2012a), suggesting that it is only important to consider the residual doses for relatively young samples (e.g., D_e < 100 Gy). Significantly higher residual doses have subsequently been reported by others (e.g., Buylaert *et al.*, 2011; Stevens *et al.*, 2011; Buylaert *et al.*, 2012; Lowick *et al.*, 2012). Some exceptions were also reported by Reimann and Tsukamoto (2012) who found that the residual doses associated with the 50°C IRSL and pIRIR(150) signals were the same after a prolonged bleach, although the pIRIR signal has been shown to bleach more slowly than the 50°C IRSL signal.

In **Fig. 5a**, all published residual doses for the pIRIR(50, 290), pIRIR(50, 225) and the 250°C MET-pIRIR signals are summarized for a range of different samples from different geographical regions and depositional environments. All the data are also summarized and referenced in **Table S1**. Large variation in the residual doses of the pIRIR signals can be seen in **Fig. 5a**. For the pIRIR(50, 290) signal, the majority of the samples studied have residual doses lower than ~35 Gy, but there are 10 samples from Switzerland (Lowick *et al.*, 2012) yielding high residual doses of between ~39 and 145 Gy. Residual doses up to ~60 Gy were also reported for the pIRIR(50, 225) signal. Again, the highest values are all reported for the 10 waterlain sediments from Switzerland ranging between ~13 and 53 Gy (Lowick *et al.*, 2012). Most of the rest of the samples have residual doses of less than ~17 Gy. The pIRIR(50, 225) signal, thus, appears to have smaller residual doses compared to the pIRIR(50, 290) signal. We note that the residual doses reported in published papers (**Table S1**) were measured using different bleaching methods and a variety of durations, which could result in different residual doses. However, many of the largest residual doses reported were obtained from samples given the most extensive bleaches. For example, Lowick *et al.* (2012) bleached their samples using a 24 h exposure to a Sunlux Ambience UV lamp, and Stevens *et al.* (2011) bleached their samples using daylight for many days. In contrast, many of the samples with smaller residual doses were bleached for only a few hours (e.g., Li and Li, 2011a; Buylaert *et al.*, 2012). We propose, therefore, that the observed variability in residual dose (**Fig. 5**) is due mainly to sample-to-sample variation, rather than different bleaching conditions used.

Large variation in the residual doses of the MET-pIRIR signals have also been observed, ranging from a few Gy to ~30 Gy (**Table S1**). We have plotted in **Fig. 5b** the residual doses of the MET-pIRIR signals for different samples from different regions as a function of IR stimulation temperature. Considerable variation in the residual doses for samples from different locations and at different IR stimulation temperatures can be seen. For all samples, the smallest residual doses (up to a few Gy) were obtained at an IR stimulation temperature of 50°C, and the

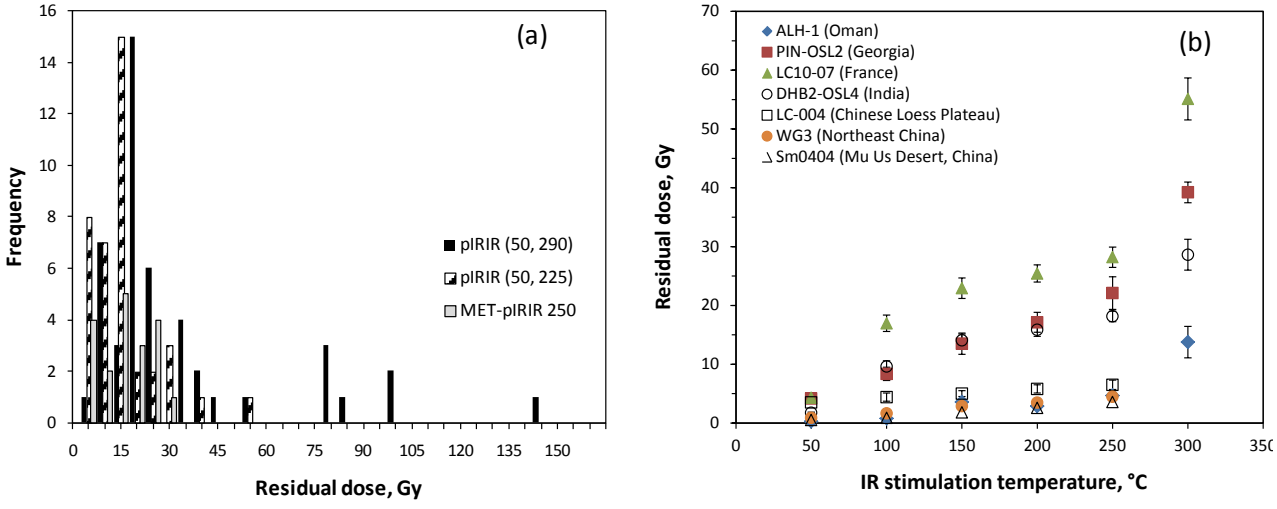

Fig. 5. *(a) A summary of all published residual dose estimates for the pIRIR(50, 290) and pIRIR(50, 225) signals for a range of different samples (Table S1). (b) Residual doses for the MET-pIRIR signals for different samples from different regions plotted against IR stimulation temperature.*

size of the residual dose and the extent of variation (in Gy) both increase with an increase in stimulation temperature (e.g., the residual doses range between ~15 and 55 Gy for the MET-pIRIR signal of 4 samples measured at 300°C). From the results of **Fig. 5**, it is clear that the residual dose associated with the non-bleachable component is highly variable from sample to sample and from site to site. This highlights the importance of obtaining accurate and precise constraints on the residual dose, even for old samples, especially when stimulated at elevated temperatures.

A strong correlation between D_e and residual dose has also been reported by some authors where samples with higher D_e values tend to have higher residual doses (e.g., Sohbati *et al.* (2012) and Buylaert *et al.* (2012) and Schatz *et al.* (2012) for the pIRIR(50, 290) signal). They suggested that this is due to stronger (or more prolonged) sunlight exposure in nature in the past compared to what they have used in the laboratory to conduct their bleaching experiments (*i.e.*, bleaching with a solar spectrum on a laboratory time scale did not result in a comparable residual reached in nature). It was, therefore, suggested that residual doses at $D_e = 0$ (obtained according to the plot of residual dose against D_e; see Fig. 5B in Buylaert *et al.* 2012) should represent the true residual dose. To further investigate if this phenomena is generally applicable for samples from different regions and different ages (or D_e), we have plotted in **Fig. 6a** all published residual dose estimates obtained for the pIRIR(50, 290), pIRIR(50, 225) and MET-pIRIR 250°C signals as a function of their residual-dose-corrected D_e values (D_e — residual). It is noted that 5 samples from Lowick *et al.* (2012) are not shown in **Fig. 6a**; their pIRIR(50, 290) signals were saturated and no D_e values were obtained. From **Fig. 6a**, it appears that there is a positive correlation between the residual dose and residual-corrected D_e values for some samples, and that this correlation is site specific. For example, the residual dose of the 5 samples of Lowick *et al.* (2012) could range from ~38 to ~80 Gy with corresponding D_e values from ~40 to ~500 Gy for the pIRIR(50, 290) signal. For the Romanian loess samples, however, the residual dose only increase from ~11 Gy to ~33 Gy with corresponding D_e values ranging from ~50 Gy to ~1600 Gy. Furthermore, residual doses ranging from a few Gy to over 50 Gy was also reported for modern samples (shown on the y-axis of **Fig. 6a**), suggesting that samples with small D_e values do not necessarily have small residual doses, and vice versa. This is further demonstrated in **Fig. 6b** where the ratio of the residual dose and the D_e value is plotted against the D_e value for each sample. It shows that the residual dose could be as high as ~50–100% of the measured D_e value for very young samples with low D_e values, and that the proportion of residual dose relative to D_e decrease with an increase in D_e. The 5 samples with pIRIR(50, 290) values that deviate significantly from the general pattern are those obtained by Lowick *et al.* (2012). A residual dose to D_e ratio less than 5% cannot be guaranteed even for samples with a D_e as high as ~500 Gy. We, therefore, suggest that sunlight or SOL2 bleaching tests might be a convenient way to obtain a minimum residual dose estimate for samples specific to each study site, and that it should be routinely conducted, even for old samples.

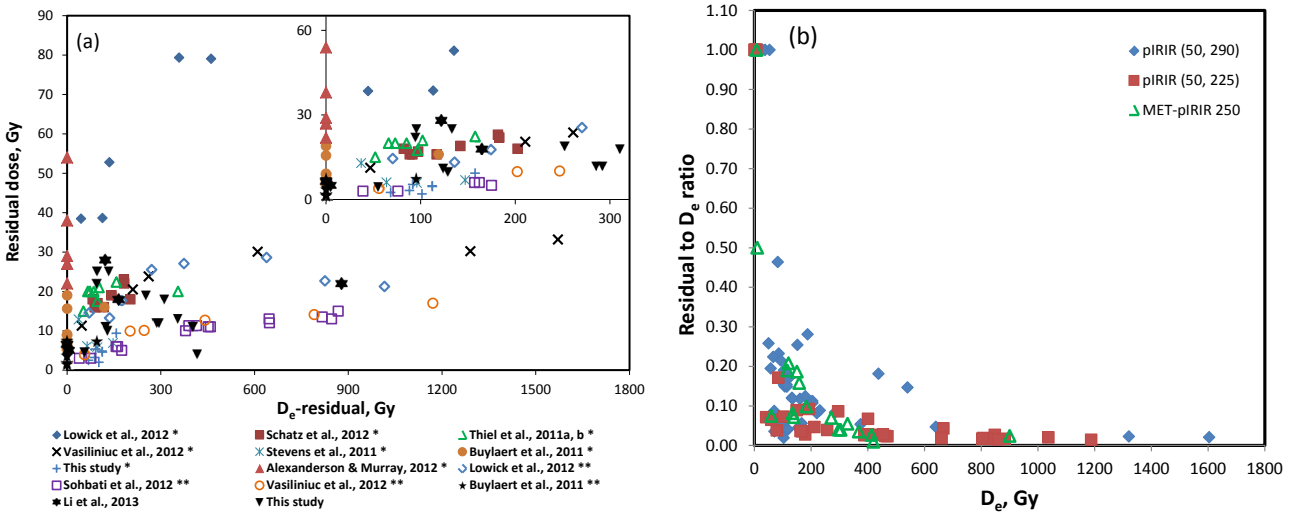

Fig. 6. *(a) The relationship between residual-corrected D_e values and residual doses for the pIRIR(50, 290), pIRIR(50, 225) and MET-pIRIR 250°C signals of different samples (see Table S1 for original data). The inset shows the enlarged scale for D_e values smaller than 320 Gy. The pIRIR(50, 290) and pIRIR(50, 225) results are marked by * and ** following the legend of each study, respectively. The MET-pIRIR(250) results are not marked. (b) The residual dose to D_e ratio plotted against the D_e value for each sample presented in (a).*

As demonstrated by the data from previous studies, the residual dose appears to be a common phenomenon for pIRIR signals (**Fig. 6a**). The source of the residual signal is, however, still poorly understood, because of the difficulty to distinguish between the non-bleachable and thermally transferred signals. The correlation between residual dose and D_e observed for some samples (e.g., Sobhati *et al.*, 2012; Buylaert *et al.*, 2012) may indicate that thermal transfer might play an important role in the production of residual signals. However, such a relationship may also be explained as a result of the dose dependency of a non-bleachable signal with an increase in natural dose. This dose dependence of the residual signal has previously been reported by Li *et al.* (2013). For unheated sediments, the traps associated with the non-bleachable signal are expected to be in dose saturation due to the long geological history of the grains (e.g., millions of years). As a result, young samples should have the same residual dose as older samples, if the samples have the same proportion of non-bleachable and bleachable traps. However, this condition is not guaranteed for all the sediments. It is very likely that the non-bleachable traps of some grains could have been reset by heat before burial due to, for example natural fires, volcanic eruptions *etc.*, which commonly occur in nature. After burial, these traps are then re-filled by exposure to naturally-occurring ionising radiation. If this is the case then older sediments will have a higher residual dose.

No matter which source the residual signal is from, it has to be corrected for appropriately for young samples and even for some old samples (**Fig. 6a** and **6b**). The most straightforward method is to subtract the residual dose obtained by directly bleaching the natural sample from the corresponding D_e values. This method will, however, result in underestimation, as demonstrated mathematically by Li *et al.* (2013). This problem can be overcome by applying an 'intensity-subtraction' method, proposed by Li *et al.* (2013), involving the construction of a dose response curve for the residual signal and then subtraction of the dose-dependent residual signal from the total signal. This method does not require information from modern analogues so it can be applied to the same sample that is dated. A drawback of this method is that it requires more aliquots and longer measurement time. An alternative way to deal with the residual dose problem is to establish a relationship between residual dose and D_e using a series of samples from the same study site, as proposed by Sobhati *et al.* (2012) and Buylaert *et al.* (2012), to calculate the residual dose using the intercept on the residual-dose axis and subtract this residual dose from the D_e of associated samples. This method can, however, only be applied to samples from the same site and requires that all the samples have the same luminescence behaviour and bleaching histories, and it is not applicable for the sites from which insufficient samples with different ages were available.

SAR performance

Whether a SAR protocol is appropriate for D_e measurement for a particular sample can be evaluated using several established tests, such as the recycling ratio test, degree of recuperation and a dose recovery test (Wintle and Murray, 2006). The first two tests can be obtained as part of the construction of the dose response curve, which involves measurement of a repeat dose at the end of the measurement sequence to obtain the recycling ratio, and measurement of a sensitivity-corrected zero dose that is then compared to the sensitivity-corrected natural dose to obtain an estimate of signal recuperation. The dose recovery test investigates the ability of the SAR protocol to recover a known dose given to a sample that has been optically bleached. For the IRSL and pIRIR measurements of feldspars, a similar SAR structure to quartz OSL has been used, and the same three tests adopted to evaluate their SAR performance (Wallinga *et al.*, 2000).

Recycling ratio and recuperation

In a SAR protocol, Murray and Wintle (2000) suggested that any recycling ratio of between 0.90 and 1.10 is acceptable. Based on 183 aliquots from 29 samples, Buylaert *et al.* (2009) found an overall recycling ratio of 0.996 ± 0.002 when measuring the dose using the pIRIR(50,225) signal, suggesting that the test dose is monitoring the sensitivity change appropriately for their laboratory-irradiated samples. A similar result was also reported for the pIRIR(50, 290) (Buylaert *et al.*, 2012) and MET-pIRIR signals (Li and Li, 2011a).

The effect of recuperation is usually expressed as a percentage ratio between the sensitivity-corrected zero dose signal and the sensitivity-corrected natural signal, and it was suggested that this value should not exceed 5% (Murray and Wintle, 2000). For the pIRIR(50,225) signal, an average recuperation value of $3.47 \pm 0.13\%$ ($n = 183$) was obtained by Buylaert *et al.* (2009). These authors also reported recuperation of <4% for the pIRIR(50, 290) signal for the majority of their samples (Buylaert *et al.*, 2012). For the MET-pIRIR signals, Li and Li (2011a) observed higher recuperation for the MET-pIRIR signals measured at higher temperatures. They found that the level of recuperation is also dependent on the size of the natural dose; younger samples tend to have higher recuperation because it is expressed as a fraction of the natural signal. For young samples, recuperation values for the 250°C MET-pIRIR signal are generally <5%, and the recuperation values for older samples and the lower-temperature MET-pIRIR signals are smaller. These studies suggest that recuperation of pIRIR signals are generally low and acceptable in the SAR protocols used.

Preheat temperature dependence

A preheat before OSL or IRSL measurement is required to remove any thermally unstable charge and to

mimic any charge transfer that may have occurred in nature. A suitable preheat temperature should be chosen so that it is high enough to be able to remove all the unstable charge that may escape in nature and low enough to avoid depleting the main luminescence traps used for dating and that may cause significant sensitivity change. For the pIRIR methods, a higher preheat temperature could also remove more easy-to-fade components in the subsequent IRSL signals (e.g., Jain and Ankjærgaard, 2011). Whether the preheat temperature used in the protocol is suitable or not can be tested by investigating if there is any dependence of D_e upon preheat temperature, the so-called 'preheat plateau' test (Murray and Roberts, 1998; Murray and Wintle, 2000).

Li and Li (2011a) first tested the effect of preheat temperature on the pIRIR signals using the MET-pIRIR procedure. They showed that, for their samples from northern China, there is no systematic dependence of D_e upon the preheat temperature ranging between 220 and 300°C for the MET-pIRIR signals measured at elevated temperatures (>150°C). A slight decrease of D_e at higher preheat temperatures was, however, observed for the IRSL and MET-pIRIR signals measured at lower stimulation temperatures (50 and 100°C). Reimann *et al.* (2011) conducted a preheat plateau test for pIRIR signals measured at 180°C (pIRIR(50, 180)) using a Holocene coastal sample from the Darss-Zingst peninsula. The measured D_e values appear to decrease with an increase in preheat temperature for the pIRIR(50, 180) signal. They also observed that a higher preheat temperature resulted in higher thermal transfer and recuperation. Roberts (2012) tested the effect of preheat temperature on the pIRIR signals using loess samples from Alaska. She reported a strong dependence of D_e with changes in preheat; D_e values increased significantly with preheat temperatures above 280°C, and a plateau region was only observed between 250 and 280°C. Based on dose recovery test results and comparisons with independent ages, Roberts (2012) concluded that a high preheat temperature (>300°C) will result in significant overestimation of D_e for her samples. The results obtained using preheat temperatures of between 250 and 300°C gave reliable age estimates. She, thus, suggested that the preheat temperature is the primary driver of a change in D_e estimation rather than the pIRIR stimulation temperature. More studies are required to test whether this is a common phenomenon for different samples from different regions. These studies, however, suggest that a preheat temperature dependency of D_e estimates should be routinely conducted for all pIRIR methods. It is noted that one cannot use the pIRIR(50,290) signal when a lower preheat temperature (<300°C) is used and this same caveat applies to the MET-pIRIR signal measured at 300°C.

Stimulation temperature dependence

The pIRIR stimulation temperature appears to play a key role in D_e estimation, and it was demonstrated in **Figs. 1**, **2** and **3** that the pIRIR(50, 225) and pIRIR(50, 290) signals may yield different results when measuring fading rates and estimating D_e values (**Fig. 1–3**) for the same samples. Apart from the pIRIR stimulation temperature, it was further argued that the stimulation temperature in the prior IR stimulation (T1) may also be an important factor (Li and Li, 2011a). Li and Li (2011a) suggested that an IR bleach at 50°C may be insufficient for removing all the easy-to-fade signals, and any remaining easy-to-fade signals will be subsequently sampled by the next post-IR measurement. This led them to propose the MET-pIRIR method in order to progressively remove the fading component (see section 3).

Thomsen *et al.* (2011) investigated the effect of prior IR stimulation temperature on thermal stability. The effect of prior IR stimulation temperature on D_e estimation was subsequently investigated by Li and Li (2012b) using samples from the Chinese Loess Plateau. They found that the pIRIR(50, 290) signal may underestimate D_e for older samples with large natural doses (>500 Gy), although it appears to yield reliable results for younger samples. They also found that such underestimation in the two-step pIRIR ages disappeared if the stimulation temperature of the prior-IR measurement was increased from 50°C to 200°C, indicating that a high stimulation temperature of the prior-IR measurement can remove the fading component more effectively. Buylaert *et al.* (2012) subsequently tested the effect of the stimulation temperature in the two-step pIRIR procedure, and they found that varying the first stimulation temperature in the range 50 to 260°C has negligible effect on D_e for their samples. However, this could be due to the fact that the samples used for their study are relatively young (<150 ka) and have relatively low D_e values (<570 Gy); the oldest sample (A19) investigated by Buylaert*et al.*, (2012) has a D_e of ~566 Gy, which is close to the dose range where consistency were observed between the pIRIR(50, 290) and pIRIR(200, 290) ages (Li and Li, 2012b). It is suggested that the effect of the stimulation temperature of the first IRSL measurement on the two-step pIRIR ages should be tested for older samples (>500 Gy) to avoid insufficient removal of the easy-to-fade component by a single low temperature IR stimulation.

Test dose dependence

In the SAR protocol for pIRIR dating (**Table 1**), a test dose is applied to monitor and correct for sensitivity change that may occur between the natural and regenerative signals. It is prudent to use a test dose as small as possible to avoid any unwanted dose-dependent effects (e.g., sensitivity change) and also to save measurement time, and it also should not be too small to ensure adequate signal intensity. The effect of the size of the test dose on D_e estimation for pIRIR dating was first investigated by Qin and Zhou (2012). It was found that the measurement of the test dose signal is influenced by the thermally-transferred signals, which may affect estima-

tion of D_e and fading rates. Based on this observation, Qin and Zhou (2012) suggested that a relatively large test dose (50–80 Gy) is preferable to minimise the effect of thermal transfer. It is noted that no high temperature clean-out was used between the different SAR cycles in Qin and Zhou (2012) that may complicate this interpretation. A contrary observation was, however, reported by Buylaert *et al.* (2012) who found no systematic change in D_e with a 3 to 4 fold change in the size of the test dose. Given the different experimental observations made for different samples, it appears that the degree of thermal transfer and sensitivity change induced by the irradiation and preheat used in test dose measurement may vary significantly from sample to sample. The choice of the size of test dose for D_e estimation should, thus, be tested and determined for each set of samples.

Dose recovery test

One critical assumption of the SAR protocol is that the test dose signal following the measurement of the natural signal accurately reflects the sensitivity of the natural signal. The validity of this assumption is usually tested using a dose recovery experiment (Murray and Roberts, 1998; Wallinga *et al.*, 2000). This test involves giving a known laboratory dose to bleached aliquots. Such a given dose is then measured as an 'unknown' dose to test if the SAR protocol can reproduce the right answer. It is to be noted that a successful dose recovery test does not guarantee an accurate D_e estimation, but a failed dose recovery test does suggest that the D_e estimation is likely to be wrong. Buylaert *et al.* (2012) provided data that contradicts this general assumption. They conducted dose recovery tests using the IR(50) signal following two different preheat temperatures, 250 and 320°C and obtained measured/given dose ratios of 0.96 ± 0.02 (n = 12) and 0.72 ± 0.02 (n = 58), respectively. This is despite obtaining D_e estimates using both temperatures that are indistinguishable from each other. They concluded that a poor dose recovery test does not necessary predict inaccurate D_e estimation (Buylaert *et al.*, 2012).

Dose recovery tests have been conducted to test the reliability of the pIRIR protocols in previous studies (see **Table S2** for a summary of the data). In **Fig. 7** we have summarised the dose recovery test results for the different pIRIR protocols: pIRIR(50,225) (n = 29), pIRIR(50, 290) (n = 47) and MET-pIRIR(250) (n = 12). Note that each measured to given dose ratio represents an average obtained for several aliquots from the same sample and that the number of aliquots varies between the different studies. **Fig. 7a** presents a histogram of the different measured to given dose ratios obtained for the three different pIRIR protocols. The ratios obtained for pIRIR(50,225) range between 0.9 and 1.3 for 28 samples except one sample showing a much higher measured to given dose ratio of 2.04 ± 0.23; this outlier was obtained for a given dose of 1200 Gy (Vasiliniuc *et al.*, 2012), similar to a natural dose from the same set of samples that was shown to be close to, or in, saturation. We ignore this value for our statisitcal analysis since this given dose is close to the saturation dose level. The measured to given dose ratios obtained for 48 samples measured using the pIRIR(50, 290) signal, ranged between 0.83 and 1.57. Again, there is one sample with a much higher ratio of 1.98, but a large standard error of ± 0.60 (Roberts, 2012); the given dose for this sample was ~300 Gy. Measured to given dose ratios using the MET-pIRIR 250°C signal has only been reported for 12 samples, and the ratios fall between 0.92 and 1.13. The overall average values of the dose

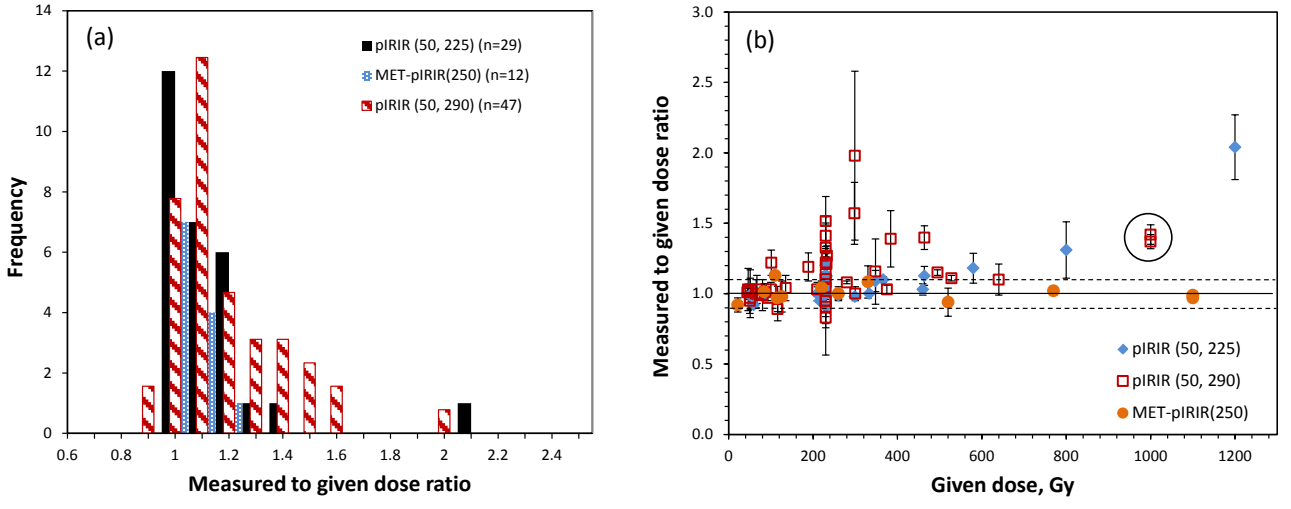

Fig. 7. *(a) Dose recovery results shown as a histogram for different pIRIR protocols (pIRIR(50,225), pIRIR(50, 290) and MET-pIRIR(250))(see Table S1 for original data). (b) The measured to given dose ratios plotted against the given dose for the same data presented in (a). Each data point represents the average value of several aliquots from the same sample. The data points from Stevens* et al. *(2011) obtained for samples that were bleached behind window glass are circled.*

recovery ratios for pIRIR(50, 225), pIRIR(50, 290) and MET-pIRIR(250) are 1.04 ± 0.01, 1.13 ± 0.03 and 1.00 ± 0.02, respectively; these averages do not include the two high outliers or those reported by Stevens *et al.* (2011) that were bleached behind window glass.

In **Fig. 7b**, the measured to given dose ratios are plotted against the given dose for all the samples summarised in **Table S2**. For the pIRIR(50, 225) signal, the recovered dose ratios are all consistent with 1.0 ± 0.1 at 1σ, except two data points obtained at 800 and 1200 Gy using the loess samples from Romania that are thought to be close to saturation (Vasiliniuc *et al.*, 2012). This suggests that the SAR protocol is suitable when measuring the pIRIR(50, 225) signal for doses smaller than 600 Gy (*i.e.*, the highest given dose for which a ratio consistent with unity was obtained).

A much larger number of samples were measured using the pIRIR(50,290) methods ($n = 47$). Thirty-three of the 47 samples gave measured to given dose ratios consistent with unity at 2σ. All, but one of the samples for which the given dose was <200 Gy was consistent with unity, but for doses >200 Gy the pattern was more inconsistent, but there do not appear to be a relationship between given dose and measured to given dose ratio (**Fig. 7b**). Those values circled in **Fig. 7b** represent the samples that were bleached behind window glass and the given dose of 1000 Gy are close to, or in, saturation. For the MET-pIRIR 250°C signal, most of the measured to given dose ratios are consistent with unity at 1σ for given doses ranging from 20 to 1100 Gy. Since there is only a small number of dose recovery tests investigated using the MET-pIRIR method, and, more importantly, no direct comparison of the MET-pIRIR and two-step pIRIR methods in the behaviour using the same set of samples, we cannot comment on the differences in the dose recovery test results. More systematic and direct comparisons of the different methods using the same samples are required.

Dose response curve

The dose response curve (DRC) determines the dose range (and, thus, age range) that can be measured for any given sample. The DRCs of IRSL and pIRIR signals are usually described by a single saturating exponential function (Thomsen *et al.*, 2008; Li and Li, 2011a):

$$I = I_0\left(1 - \exp\left(-\frac{D}{D_0}\right)\right) \quad (4.1)$$

where I is the sensitivity-corrected signal intensity, D is the regenerative dose, D_0 is the characteristic saturation dose, and I_0 is the maximum intensity at infinite dose ($D \to \infty$), or a double saturating exponential function (Buylaert *et al.*, 2012). The shape of the DRC and its saturation level are mainly controlled by the characteristic saturation dose D_0. A larger D_0 value indicates that the signal intensity will keep increasing at higher doses. Wintle and Murray (2006) suggested that a value of $2D_0$ could be taken as an conservative upper limit for dose measurement for quartz, but Li and Li (2012a) found that a reliable D_e beyond $2D_0$ can also be obtained using MET-pIRIR signal from Chinese loess samples — e.g., D_e values up to 1000 Gy were obtained using MET-pIRIR(250) signal even though the corresponding $2D_0$ value is 600–700 Gy — but a loss of precision was inevitable (Li and Li, 2012a).

The shapes of the DRCs for the IRSL and pIRIR signals were compared in a few studies (e.g., Buylaert *et al.*, 2009; Vasiliniuc *et al.*, 2012; Thiel *et al.*, 2011a; 2011b; Thomsen *et al.*, 2011; Andersen *et al.*, 2012). Buylaert *et al.* (2009) first compared the DRCs of 50°C IRSL and pIRIR(50, 225) signals for a sample from Denmark, and found that there is no difference in the DRCs up to 2000 Gy. A similar observation was reported by Sohbati *et al.* (2012). However, different shapes were observed between the 50°C IRSL and pIRIR(50, 225) signals for K-feldspar from Romanian loess (Vasiliniuc *et al.*, 2012). They also observed lower sensitivity-corrected signal intensities and an earlier dose saturation for the pIRIR(50, 225) signal. For the pIRIR(50, 290) method, Thiel *et al.* (2011a) first compared the DRCs for both the 50°C IRSL and pIRIR(50, 290) signals for their loess samples from Austria, and found indistinguishable DRCs for the two signals. However, using Japanese loess samples, Thiel *et al.* (2011b) subsequently reported an earlier saturation in the DRC of the pIRIR(50, 290) signal compared to that of the 50°C IRSL. Similar results were also reported for pIRIR(50, 300) signals from Romanian loess (Vasiliniuc *et al.*, 2012) and pIRIR(50, 245) signals from a shallow marine Eemian sample from Denmark (Thomsen *et al.*, 2011). Different DRCs of MET-pIRIR signals were also reported (Li and Li, 2011a; Fu *et al.*, 2012a; Li and Li, 2012a). Based on eolian samples from northern China, Li and Li (2011a, 2012a) found that the shapes of the DRCs differ according to stimulation temperature for the MET-pIRIR signals, with the 50°C IRSL dose response growing to the highest doses. The DRCs are similar for the signals measured at 50, 100 and 150°C, while an earlier saturation was observed for the signals measured at 200 and 250°C.

To provide an example of systematic comparison between the DRCs for different IRSL and pIRIR signals at different temperatures using the same sample, we measured the DRCs using different pIRIR methods using 6 aliquots of an aeolian sample (Sm8) from the Mu Us Desert, central China. It is noted that the behaviour of this sample may not necessarily represent the K-feldspar from other regions. **Fig. 8a** shows the DRCs using the two-step pIRIR method with various combinations of stimulation temperatures and preheat temperatures (shown in the legend). The 50°C IRSL signal, measured using the pIRIR(50, 290) method with a preheat at 320°C for 60 s, shows the highest D_0 value of 575 ± 36 Gy. The pIRIR(50, 290) signal grows indistinguishably from the

50°C IRSL signal up to ~500 Gy, but gets depressed and saturated earlier at higher dose. The influence of the prior-IR stimulation temperature on the DRC was also investigated using different prior stimulation temperatures (T1), at 100, 150 and 200°C, together with the same pIRIR stimulation temperature at 250°C and preheat at 300°C for 60 s (**Fig. 8a**). It is shown that different prior stimulation temperature (T1) results in a different sensitivity-corrected intensity, indicating a different extent of changes in response from the natural or regenerative step to the test dose measurement (Chen *et al.*, 2001; Wintle and Murray, 2006). Increasing the prior stimulation temperature also results in an earlier saturation of the signals. The saturation levels of the DRCs in **Fig. 8a** can be demonstrated more clearly when all the DRCs are normalised to a saturation value of 1 (**Fig. 8b**). This result indicates that, although increasing the prior stimulation temperature in the pIRIR procedure may yield a more stable signal (Li and Li, 2012b), it will also result in an earlier saturation of the pIRIR signal, which will limit the dating range of the pIRIR method.

The MET-pIRIR method is actually a simple combination of multiple pIRIR procedures with different prior IR stimulation temperatures, which are achievable on a single aliquot. **Fig. 8c** shows the DRCs of the MET-pIRIR signals at different IR temperatures obtained from a single aliquot of the same sample Sm8, and **Fig. 8d** shows the same set of DRCs but are normalised to a saturation value of 1. As expected, different sensitivity-corrected DRCs was observed for different IRSL and

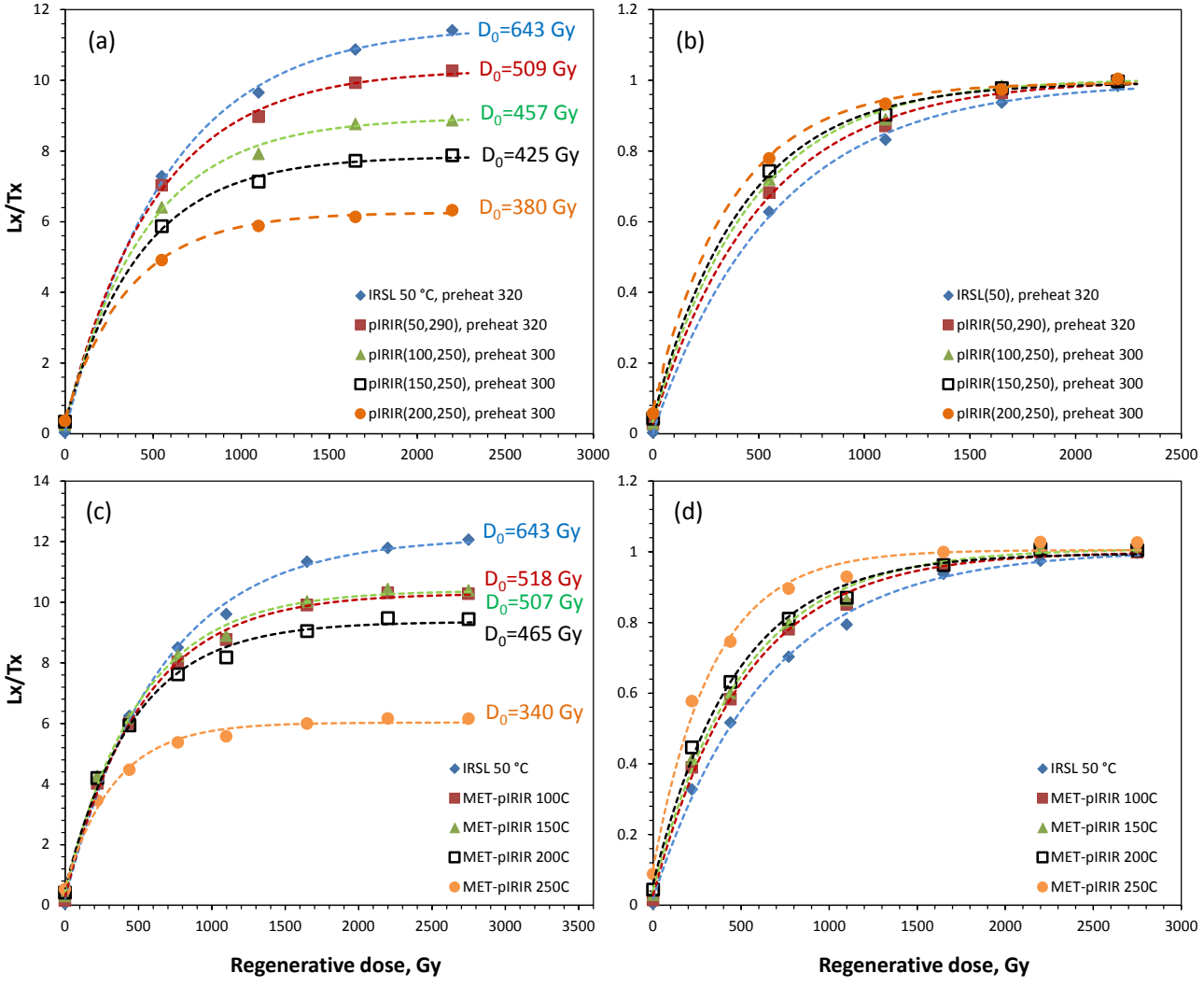

Fig. 8. *(a) The DRCs of sample Sm8 obtained using a range of different two-step pIRIR protocols (measurement conditions shown in legend). (b) The same data sets as (a) but all the curves were normalised to a saturation value of 1. (c) The DRCs of sample Sm8 obtained using the MET-pIRIR method with a preheat of 300°C. (d) The same data sets as (c) but all the curves were normalised to a saturation value of 1. The dashed lines are the best-fit curves using a single exponential saturating function. The values of the characteristic saturation dose (D_0) obtained for each DRC are shown next to each curve in (a) and (c).*

MET-pIRIR signals. The 50°C IRSL signal yielded the highest sensitivity-corrected intensity and the highest saturation dose (D_0 = 643 ± 37 Gy). The DRCs for the 100 and 150°C signals are indistinguishable and have a similar D_0 value of ~510 Gy. The 200 and 250°C signals have lower intensities and lower D_0 values of 465 and 340 Gy, respectively. The results of the MET-pIRIR signals shown in **Fig. 8c** are very similar to the results of the pIRIR methods with different prior stimulation temperatures shown in **Fig. 8a**.This suggests that the shape and characteristic saturation dose of the DRCs of pIRIR signals is mainly determined by the prior stimulation temperature — a higher prior stimulation temperature will result in earlier saturation of the DRC.

According to the results of **Fig. 8**, it appears that the pIRIR method with an elevated prior IR stimulation temperature and the MET-pIRIR method may have an upper limit of dose determination at 700–800 Gy for the samples investigated if a D_e equal to $2D_0$ is considered a conservative upper limit (Wintle and Murray, 2006; but see Galbraith and Roberts, 2012). However, variable saturation levels of the pIRIR signals for different samples from different regions of the world are possible. For example, a much higher D_0 value of ~750 Gy was observed for the pIRIR(50, 245) signal for a shallow marine Eemian sample from Denmark (Thomsen *et al.*, 2011). Stevens *et al.* (2011) reported much lower D_0 values (<200 Gy) using the pIRIR(50, 290) method for their loess samples from the Carpathian Basin in Europe, but the maximum dose given in their DRC is ~400 Gy, which limits the reliability of determining the true saturation dose level. Gliganic *et al.* (2012) obtained a D_0 value of ~350 Gy using the pIRIR(50, 225) method for their archaeological samples from Tanzania. Kars *et al.* (2012) obtained D_0 values of ~400–500 Gy using the pIRIR(100, 230) method for sediments from Netherlands.

In conclusion, the dating limit of the pIRIR method may be highly variable from sample to sample and region to region but the saturation dose level is highly dependent on the experimental condition used (e.g., prior IR stimulation temperature and the pIRIR stimulation temperature).

5. AGE COMPARISON WITH INDEPENDENT AGES

Although demonstrating that the SAR protocol performs reliably, using such tests as the recycling ratio, recuperation, preheat plateau, anomalous fading and dose recovery tests, the most important test of the reliability of any dating technique is whether it can yield consistent results when compared with ages for the same sample or context obtained using an independent dating technique. We provided in **Table S1** the independent ages (*i.e.*, 'expected age') for all published pIRIR ages where such ages were reported. The majority of samples for which independent ages were available range in age from 0 to 400 ka, except for one sample of Japanese loess (Tg22) for which a quartz OSL age 507 ± 41 ka and a fission track age of 660 ± 40 ka is known (Watanuki *et al.*, 2005). Independent age control for the rest of the samples came from predominantly quartz OSL, but also from radiocarbon, fission track, tephra chronology and also stratigraphic correlation and paleomagnetism. We did not attempt to assess the quality of the independent ages for each of the samples, but rather assumed that the reliability of the independent ages was verified by the respective authors of each study.

Fig. 9 shows the fading-uncorrected pIRIR ages compared to independent ages for the three pIRIR methods that have been tested most extensively; pIRIR(50, 225) (**Fig. 9a** and **9b**), pIRIR(50, 290) (**Fig. 9c** and **9d**) and MET-pIRIR 250°C (**Fig. 9e** and **9f**). We also show as open symbols in **Fig. 9a** and **9b** the fading-corrected pIRIR(50, 225) ages for the same samples. We have done this to reflect the current trend to correct the pIRIR(50, 225) ages, but not the pIRIR(50, 290) ages for fading (see discussion above). The figures in the left-hand column show the entire age range, whereas those in the right-hand column only show the samples younger than 100 ka for clarity. We have also summarised in **Table 2** the percentage of samples that have pIRIR ages consistent with their independent ages at 1 and 2σ. Since a primary purpose of the development of the pIRIR dating procedure is to extend the dating range to older samples (>100 ka), we have divided the samples into two groups; one group is for samples older than 100 ka, and the other is from samples with ages between 20 and 100 ka. It is noted that in **Table 2** we purposely ignored those samples

Table 2. *The fraction of the samples that have pIRIR ages that are consistent with their independent ages for different methods. The number of samples (n) summarised for each method is shown.*

Method	20–100 ka		>100 ka		>20 ka	
	1σ	2σ	1σ	2σ	1σ	2σ
pIRIR(50, 225), n = 38 (Fading uncorrected)	57%	86%	21%	38%	34%	55%
pIRIR(50, 225), n = 38 (Fading corrected)	57%	64%	33%	63%	42%	63%
pIRIR(50, 290), n = 95	57%	81%	41%	73%	51%	78%
MET-pIRIR 250, n = 30	76%	94%	77%	100%	77%	97%
All methods, n = 197	61%	85%	41%	64%	51%	74%

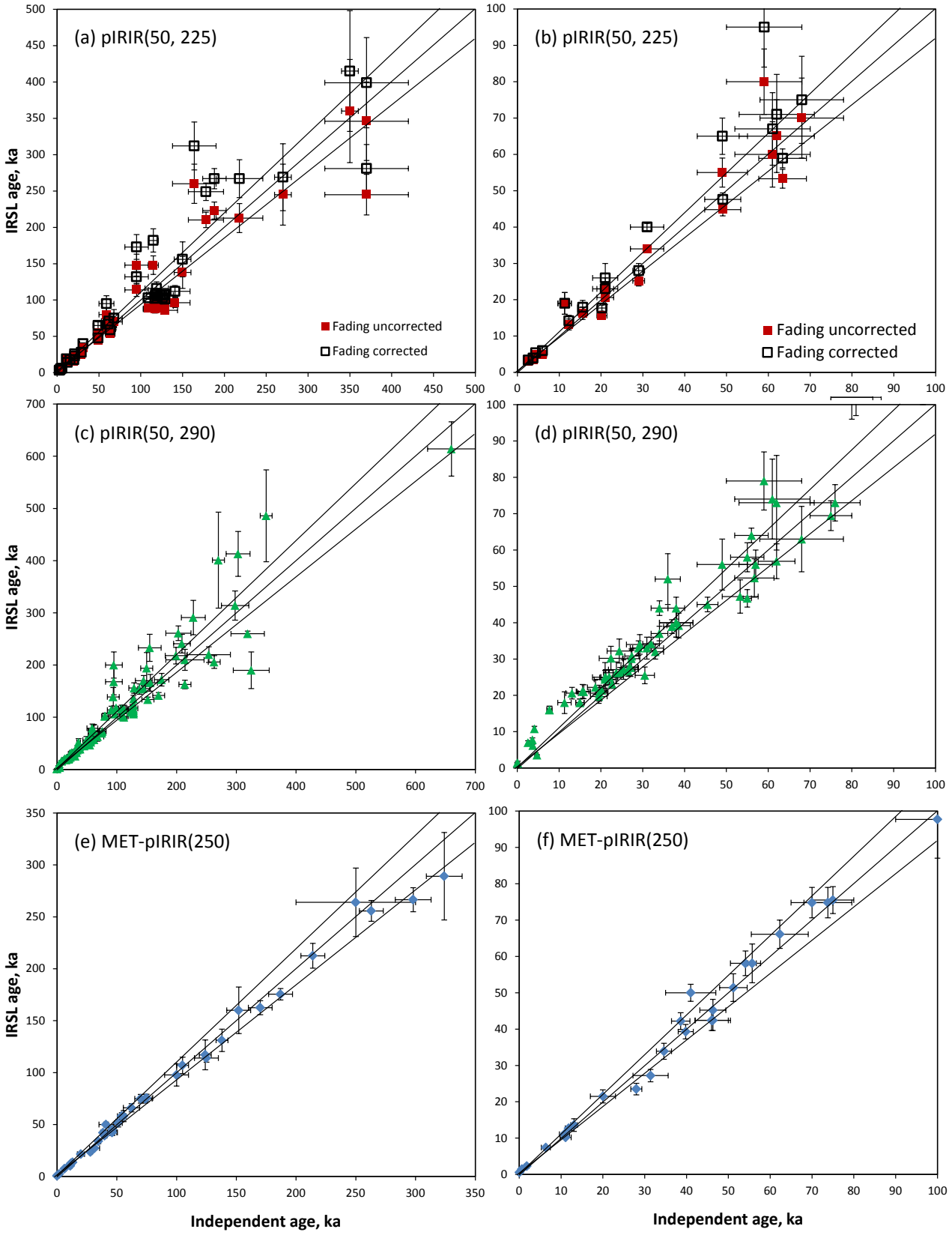

Fig. 9. *Comparisons of independently obtained ages and the pIRIR ages for samples summarized in Table S1 obtained using (a) the pIRIR(50, 225) signal (fading corrected and uncorrected ages), (c) the pIRIR(50, 290) signal, and (e) the MET-pIRIR 250°C signal. (b), (d) and (f) show the same data sets as (a), (c) and (e), respectively, but only for younger samples on an enlarged scale.*

younger than 20 ka to avoid significant influence on the statistics from issues associated with the measurement and subtraction of the residual dose for young samples.

There are 47 samples with independent ages that were measured using the pIRIR(50, 225) method; 45 are shown in **Fig. 9a** and 2 samples, reported by Lowick *et al.* (2012), gave minimum ages that were excluded from this analysis as these were in, or close to, saturation. Of the 45 samples, 7 gave ages <20 ka, 14 are between 20 and 100 ka old, and 24 samples gave ages older than 100 ka (**Table S1**). All 45 ages (fading-corrected and fading-uncorrected) are plotted against their respective independent age estimates in **Fig. 9a** and **9b**. Taking into account all 45 samples, 58% of the fading-uncorrected pIRIR(50, 225) ages, and 64% of the fading-corrected ages, are consistent with their independent ages at 2σ (**Table 2**; **Fig. 9b**). For those samples with ages between 20 and 100 ka (n = 14), 86% are consistent at 2σ, but this decreases to 64% when the ages are corrected for fading. All the samples with fading-corrected ages that are inconsistent with their independent ages at 2σ are those reported in Lowick *et al.* (2012) and these consistently overestimate their known ages. These samples had a residual dose subtracted prior to calculation of the ages, but since these ages are for waterlain sediments, inhomogeneous bleaching of the pIRIR signal may have led to age overestimation. If we ignore the 5 samples from Switzerland (Lowick *et al.*, 2012), all but one sample (*i.e.*, 8 out of 9) have fading-uncorrected ages consistent with the expected ages, and all samples (n = 9) have fading-corrected ages consistent with the expected ages. Accordingly, there is no clear advantage of applying a fading-correction for the pIRIR(50, 225) signal for the samples in this age group (20–100 ka).

For those samples with ages >100 ka (n = 24), 38% (uncorrected) or 63% (fading-corrected) are consistent with their independent ages at 2σ (**Fig. 9a**). Fading correction appears to improve the consistency between the pIRIR ages and the expected ages for these samples, but we reserve our judgment on the validity of the fading-corrected ages because of the limitation of the correction method to older samples (Huntley and Lamothe, 2001). The majority of the samples with fading-uncorrected ages inconsistent with their independent ages at 2σ are those reported by Buylaert *et al.* (2012) for coastal sediment samples from Denmark and Russia. The coastal sand samples from Denmark with independent ages of ~110–130 ka gave fading-uncorrected pIRIR ages that are consistently underestimated, whereas the coastal sediment samples from Russia with independent ages of between 115 and 218 ka gave pIRIR ages that appear to either underestimate (n = 6) or overestimate (n = 3) their known ages. So, on average, there is no systematic over- or under-estimation of the fading-uncorrected pIRIR ages relative to their known ages and no average trend with age can be observed; the results are most likely sample-dependent.

There are 121 samples with independent ages that were measured using the pIRIR(50, 290) method; 116 of these are shown in **Fig. 9c** and 5 samples, all reported by Lowick *et al.* (2012), were omitted because they were reported as minimum ages without error estimates and had signals that were in, or close to, saturation. Of the 116 samples, 23 gave expected ages <20 ka, 52 fell between 20 and 100 ka, and 41 samples gave ages older than 100 ka (**Table S1**). Whether or not a residual-dose subtraction was applied and how this residual dose was determined and subtracted varied among the different studies (see each study for relevant information). We have plotted here the final best-estimate ages reported in each study. Taking into account all 116 samples, 66% of the samples gave pIRIR(50, 290) ages consistent with their independent ages at 2σ (**Table 2**; **Fig. 9b**); this increase significantly to 77% if we omit the 25 samples with ages <20 ka. These samples were not corrected for residual doses since many of these were used to obtain an estimate of the residual dose. For those samples with ages between 20 and 100 ka (n = 52), 81% are consistent at 2σ; the 19% (n = 10) of samples with inconsistent ages all (except for one sample) have pIRIR ages that overestimate their known age. These samples come from a range of different geographical areas, including Egypt, Tunisia, Japan and Europe and represent different depositional environments, including coastal sand, aeolian dunes, loess and waterlain sediment. Six of these samples, from Thiel *et al.* (2011b; 2012) and Stevens *et al.* (2011), had not been corrected for any residual dose prior to pIRIR age determination. Residual doses of up to 20 Gy were observed for the Japanese samples (Thiel *et al.*, 2011b). We note that if we subtract a residual dose of 20 Gy from their D_e values, the pIRIR ages are consistent with the expected ages for these samples. Age overestimation is also removed after subtracting the residual dose (32.8 Gy) measured for the sample of Stevens *et al.* (2011). For the two waterlain samples from Switzerland (Lowick *et al.*, 2012), age overestimation was observed even after subtraction of the residual doses, but this could be due to insufficient bleaching prior to deposition. We cannot assess the reason for age overestimation of the sample from Egypt (Buylaert *et al.*, 2012), because residual dose was not reported for this sample.

For those samples with ages >100 ka (n = 41), 73% are consistent at 2σ. Eight of the 11 samples that are inconsistent have pIRIR ages that are underestimated relative to their known ages and only three are overestimated. This is in contrast to the ages obtained for samples between 20 and 100 ka. So, like the pIRIR(50,225) ages, there does not appear to be a systematic trend and the differences are probably sample dependent, but for younger samples (between 20 and 100 ka) it appears that estimation of an accurate and site-specific residual dose is critical. For the older samples (>100 ka), a small amount of fading, consistent with the average fading rate of ~1.1%/decade (**Fig. 2**), may be more important than the

residual dose. In other words, these two factors may work against each other, depending on the age of the sample and the relative size of the residual dose and the fading rate. Other effects, such as thermal stability, preheat temperature dependence, test dose dependence and sensitivity correction (see section 4) may also contribute to the spread in ages.

There are 38 samples with independent ages that were measured using the MET-pIRIR 250°C signal; ages for all 38 samples are presented in **Fig. 9e**. The MET-pIRIR method has been tested primarily for aeolian samples from northern China (Li and Li, 2011a, 2012a; Fu *et al.*, 2012a) (see **Table S1**). Of the 38 samples, 8 gave ages <20 ka, 17 are between 20 and 100 ka old, and 13 samples gave ages older than 100 ka (**Table S1**). No fading correction was applied to any of the ages and measured residual doses were subtracted from each sample D_e value prior to age calculation. Taking into account all 38 samples, 95% of the samples gave ages consistent with their independent ages at 2σ (**Table 2**; **Fig. 9e**). There is no significant difference in the number of samples that are consistent with their independent ages for those samples that are between 20 and 100 ka (94% at 2σ; **Fig. 9f**) and those older than 100 ka (100% at 2σ). The method appears to be reliable for most of the samples from this region and for samples as old as ~300 ka. However, since most of these data are limited to samples from northern China that are expected to have similar luminescence behaviors, more studies from other regions of the world are required to test the broader applicability of the MET-pIRIR method.

Fig. 10a and **10b** summarise all the feldspar IRSL ages presented in **Fig. 9** together with those that utilised slightly different pIRIR approaches (see legend in **Fig. 10a**). It demonstrates that regardless of which pIRIR method is used, excellent agreement is obtained between the fading-uncorrected pIRIR ages and their independent ages for the samples between 20 and 100 ka (**Fig. 10b**); this consistent pattern falls apart for older samples (>100 ka) (**Fig. 10a**). For samples between 20 to 100 ka, 85% of the samples are consistent with their independent ages at 2σ (**Table 2**). For the older samples (>100 ka), only 64% of the samples yielded ages consistent with their independent ages at 2σ, and both over- or underestimated ages are obtained for the rest of the samples (**Fig. 10a**).

In summary, the dating results using various pIRIR protocols are sensitive to the procedure and experimental conditions chosen. All the different variations of the pIRIR methods, however, appear to yield reliable ages for relatively young samples (20–100 ka), but the reliability for dating older samples is not guaranteed and both under- and overestimation may be obtained.

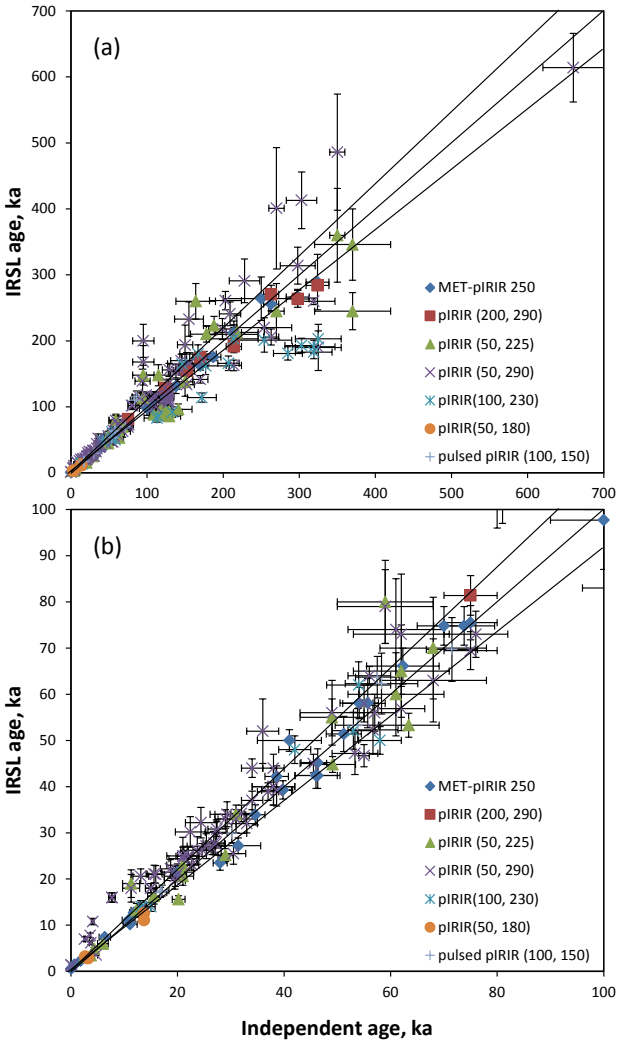

Fig. 10. *(a) A summary of the feldspar pIRIR ages obtained using various pIRIR methods with comparison to the independent ages (see Table S1 for original data). (b) The data sets for samples younger than 100 ka only.*

6. SUMMARY

The discovery of the fading-immune feature of the pIRIR signal and development of various pIRIR procedures has, for the first time, provided an effective way to overcome anomalous fading in feldspar. The pIRIR method does not only allow an extension of the age limit of luminescence dating, but also allow dating of sediments in which little quartz grains are found or that contain quartz grains with unwanted OSL behaviours. It, thus, opened up a new era of luminescence dating of sediments using feldspars. Although promising results have been reported by a number of published studies, important problems have been reported and remain unanswered:

1) Many of the fading-uncorrected pIRIR ages agree with independent age control. This agreement, however, is inconsistent with the non-zero apparent laboratory fading rates. For ages that are either underestimated or overestimated, it is not clear whether this inconsistency is a result of the observed fading rate or the D_e estimate, or both, being an artefact.
2) A complex and variable SAR performance of the pIRIR signals has been observed for different samples from different regions. The choice of preheat temperature appears to be critical for some samples, but not for all. The dependence of IR stimulation temperatures, either prior-IR stimulation or pIRIR stimulation temperature, was also variable from sample to sample. The effect of thermal transfer and the size of test dose could also be a potential influence on D_e estimation. All these observations suggest that there is no universal pIRIR procedure applicable to every sample. One need to conduct comprehensive experimental tests to find the best suitable pIRIR procedures for any particular set of samples.
3) The residual dose appears to be highly variable from sample to sample and from region to region (**Fig. 5–6**). The source of the residual signal is still poorly understood, which may potentially affect the accuracy of age estimation. A modern analogue may provide an estimate on the true residual dose before burial, but this does not guarantee a reliable estimate of the true residual dose. At this point in time, most studies either do not deal with the residual dose or simply subtract a residual dose from the apparent D_e value with the residual inferred from measurement of fully bleached grains of the same or different samples. The dose dependence of the residual signal and the effect of thermal treatment (or thermal transfer) require further investigation, before it can be appropriately corrected for.
4) From the published data, it appears that the application of pIRIR dating methods is most successful for samples between 20 and 100 ka. However, it was less successful for older samples (e.g., >100 ka), where the pIRIR dating method is most useful compared to quartz OSL dating.

In summary, we reiterate previous suggestions that a preheat plateau test, residual signal measurements, a fading rate test, and dose recovery tests should be conducted as minimum criteria to validate the reliability of any pIRIR procedure. These tests, however, do not necessarily guarantee the accuracy of dating results, but can provide useful insights into the sensitivity of samples to different parameters of the method. Given the fact that the published studies are more likely to be dominant by successful application of pIRIR dating, and failed attempts of pIRIR dating is less likely to be published, the results summarised in this study is probably biased to successful applications and, therefore, should be regarded as an optimistic review. Finally, dating more sites, where independent age controls are available, is required.

ACKNOWLEDGEMENTS

The authors thank the two anonymous reviewers for their thorough reviews and constructive comments. We thank the organisation committee of the 3rd APLED conference held at the University of Okayama, Japan, in 2012 for inviting us to present this review. Sally Lowick is appreciated for providing raw data from Lowick *et al.* (2012). This study was supported by a University of Wollongong Vice-Chancellor's Postdoctoral Research Fellowship to B Li, by Australian Research Council grants and fellowships to Roberts (DP0880675) and Jacobs (DP1092843), and by the Research Grant Council of the Hong Kong Special Administrative Region, China, to SHL (7033/12P).

APPENDIX

Two figures and two tables are available as Supplementary Material in electronic version of this article at http://dx.doi.org/10.2478/s13386-013-0160-3. **Fig. S1**: Solar simulator bleaching experiments for IRSL and pIRIR signals reported by (A) Buylaert *et al.* (2012) and (B) Li and Li (2011a). **Fig. S2**: Anomalous fading rates (g-values) for the MET-pIRIR signals of a sample (HLD-3) from northeast China, plotted against stimulation temperature (data from Li and Li, 2011a). **Table S1**: Summary of the pIRIR dating results from recently published studies using different pIRIR procedures. **Table S2**: Summary of the pIRIR dose recovery results from recently published and unpublished studies using different pIRIR procedures.

REFERENCES

Aitken MJ, 1985. *Thermoluminescence dating*. Academic press, London.

Aitken MJ, 1998. An Introduction to Optical Dating. Oxford University Press. London, 267 pp.

Alappat L, Tsukamoto S, Singh P, Srikanth D, Ramesh R and Frechen M, 2010. Chronology of Cauvery Delta Sediments from Shallow Subsurface Cores Using Elevated-Temperature Post-Ir Irsl Dating of Feldspar. *Geochronometria* 37: 37–47, DOI 10.2478/v10003-010-0025-1.

Andersen MT, Jain M and Tidemand-Lichtenberg P, 2012. Red-IR stimulated luminescence in K-feldspar: Single or multiple trap origin? *Journal of Applied Physics* 112: 043507, DOI 10.1063/1.4745018.

Auclair M, Lamothe M and Huot S, 2003. Measurement of anomalous fading for feldspar IRSL using SAR. *Radiation Measurements* 37(4–5): 487–492, DOI 10.1016/S1350-4487(03)00018-0.

Baril MR and Huntley DJ, 2003. Infrared stimulated luminescence and phosphorescence spectra of irradiated feldspars. *Journal of Physics: Condensed Matter* 15(46): 8029–8048, DOI 10.1088/0953-8984/15/46/018.

Buylaert JP, Jain M, Murray AS, Thomsen KJ, Thiel C and Sohbati R, 2012. A robust feldspar luminescence dating method for Middle

and Late Pleistocene sediments. *Boreas* 41(3): 435–451, DOI 10.1111/j.1502-3885.2012.00248.x.

Buylaert JP, Murray AS, Thomsen KJ and Jain M, 2009. Testing the potential of an elevated temperature IRSL signal from K-feldspar. *Radiation Measurements* 44(5–6): 560–565, DOI 10.1016/j.radmeas.2009.02.007.

Buylaert JP, Thiel C, Murray AS, Vandenberghe DAG, Yi SW and Lu HY, 2011. IRSL and post-IR IRSL residual doses recorded in modern dust samples from the Chinese Loess Plateau. *Geochronometria* 38(4): 432–440, DOI 10.2478/s13386-011-0047-0.

Chen G, Murray AS and Li SH, 2001. Effect of heating on the quartz dose-response curve. *Radiation Measurements* 33(1): 59–63, DOI 10.1016/S1350-4487(00)00134-7.

Chen YW, Li SH and Li B, 2013. Residual doses and sensitivity change of post IR IRSL signals from potassium feldspar under different bleaching conditions. *Geochronometria* 40(4): 229–238, DOI 10.2478/s13386-013-0128-3.

Fu X, Li B and Li SH, 2012a. Testing a multi-step post-IR IRSL dating method using polymineral fine grains from Chinese loess. *Quaternary Geochronology* 10: 8–15, DOI 10.1016/j.quageo.2011.12.004.

Fu X and Li SH, 2013. A modified multi-elevated-temperature post-IR IRSL protocol for dating of Holocene sediments using K-feldspar. *Quaternary Geochronology* 17: 44–54, DOI 10.1016/j.quageo.2013.02.004.

Fu X, Zhang JF and Zhou LP, 2012b. Comparison of the properties of various optically stimulated luminescence signals from potassium feldspar. *Radiation Measurements* 47(3): 210–218, DOI 10.1016/j.radmeas.2011.12.007.

Galbraith RF, Roberts RG, Laslett GM, Yoshida H and Olley JM, 1999. Optical dating of single and multiple grains of quartz from Jinmium rock shelter, northern Australia, part 1, Experimental design and statistical models. *Archaeometry* 41(2): 339–364, DOI 10.1111/j.1475-4754.1999.tb00987.x.

Galbraith RF and Roberts RG, 2012. Statistical aspects of equivalent dose and error calculation and display in OSL dating: an overview and some recommendations. *Quaternary Geochronology* 11: 1–27, DOI 10.1016/j.quageo.2012.04.020.

Gliganic LA, Jacobs Z, Roberts RG, Dominguez-Rodrigo M and Mabulla AZP, 2012. New ages for Middle and Later Stone Age deposits at Mumba rockshelter, Tanzania: Optically stimulated luminescence dating of quartz and feldspar grains. *Journal of Human Evolution* 62(4): 533–547, DOI 10.1016/j.jhevol.2012.02.004.

Guérin G and Valladas H, 1980. Thermoluminescene dating of volcanic plagioclases. *Nature* 286: 697–699, DOI 10.1038/286697a0.

Huntley DJ, 2011. Comment on "Isochron dating of sediments using luminescence of K-feldspar grains" by B. Li *et al. Journal of Geophysical Research: Earth Surface* 116(F1): F01012, DOI 10.1029/2010JF001856.

Huntley DJ and Lamothe M, 2001. Ubiquity of anomalous fading in K-feldspars and the measurement and correction for it in optical dating. *Canadian Journal of Earth Sciences* 38(7): 1093–1106, DOI 10.1139/e01-013.

Huntley DJ and Lian OB, 2006. Some observations on tunnelling of trapped electrons in feldspars and their implications for optical dating. *Quaternary Science Reviews* 25(19–20): 2503–2512, DOI 10.1016/j.quascirev.2005.05.011.

Hütt G, Jaek I and Tchonka J, 1988. Optical dating: K-feldspars optical response stimulation spectra. *Quaternary Science Reviews* 7(3–4): 381–385, DOI 10.1016/0277-3791(88)90033-9.

Jain M and Ankjærgaard C, 2011. Towards a non-fading signal in feldspar: insight into charge transport and tunnelling from time-resolved optically stimulated luminescence. *Radiation Measurements* 46(3): 292–309, DOI 10.1016/j.radmeas.2010.12.004.

Jain M and Singhvi AK, 2001. Limits to depletion of blue-green light stimulated luminescence in feldspars: implications for quartz dating. *Radiation Measurements* 33(6): 883–892, DOI 10.1016/S1350-4487(01)00104-4.

Kars RH, Busschers FS and Wallinga J, 2012. Validating post IR-IRSL dating on K-feldspars through comparison with quartz OSL ages. *Quaternary Geochronology* 12: 74–86, DOI 10.1016/j.quageo.2012.05.001.

Kars RH, Wallinga J and Cohen KM, 2008. A new approach towards anomalous fading correction for feldspar IRSL dating - tests on samples in field saturation. *Radiation Measurements* 43(2–6): 786–790, DOI 10.1016/j.radmeas.2008.01.021.

Lamothe M and Auclair M, 1997. Assessing the datability of young sediments by IRSL using an intrinsic laboratory protocol. *Radiation Measurements* 27(2): 107–117, DOI 10.1016/S1350-4487(96)00140-0.

Lamothe M and Auclair M, 1999. A solution to anomalous fading and age shortfalls in optical dating of feldspar minerals. *Earth and Planetary Science Letters* 171(3): 319–323, DOI 10.1016/S0012-821X(99)00180-6.

Lamothe M, Auclair M, Hamzaoui C and Huot S, 2003. Towards a prediction of long-term anomalous fading of feldspar IRSL. *Radiation Measurements* 37(4–5): 493–498, DOI 10.1016/S1350-4487(03)00016-7.

Li B and Li SH, 2008. Investigations of the dose-dependent anomalous fading rate of feldspar from sediments. *Journal of Physics D-Applied Physics* 41: 225502, DOI 10.1088/0022-3727/41/22/225502.

Li B and Li SH, 2011a. Luminescence dating of K-feldspar from sediments: A protocol without anomalous fading correction. *Quaternary Geochronology* 6(5): 468–479, DOI 10.1016/j.quageo.2011.05.001.

Li B and Li SH, 2011b. Thermal stability of infrared stimulated luminescence of sedimentary K-feldspar. *Radiation Measurements* 46(1): 29–36, DOI 10.1016/j.radmeas.2010.10.002.

Li B and Li SH, 2012a. Luminescence dating of Chinese loess beyond 130 ka using the non-fading signal from K-feldspar. *Quaternary Geochronology* 10: 24–31, DOI 10.1016/j.quageo.2011.12.005.

Li B and Li SH, 2012b. A reply to the comments by Thomsen *et al.* on "Luminescence dating of K-feldspar from sediments: A protocol without anomalous fading correction". *Quaternary Geochronology* 8: 49–51, DOI 10.1016/j.quageo.2011.10.001.

Li B and Li SH, 2013. The effect of band-tail states on the thermal stability of the infrared stimulated luminescence from K-feldspar. *Journal of Luminescence* 136: 5–10, DOI 10.1016/j.jlumin.2012.08.043.

Li B, Li SH and Wintle AG, 2008a. Overcoming environmental dose rate changes in luminescence dating of waterlain deposits. *Geochronometria* 30: 33–40, DOI 10.2478/v10003-008-0003-z.

Li B, Li SH, Wintle AG and Zhao H, 2007a. Isochron measurements of naturally irradiated K-feldspar grains. *Radiation Measurements* 42(8): 1315–1327, DOI 10.1016/j.radmeas.2007.09.008.

Li B, Li SH, Wintle AG and Zhao H, 2008b. Isochron dating of sediments using luminescence of K-feldspar grains. *Journal of Geophysical Research: Earth Surface* 113(F2): F02026, DOI 10.1029/2007JF000900.

Li B, Li SH and Zhao H, 2011. Reply to comment by Huntley on "Isochron dating of sediments using luminescence of K-feldspar grains". *Journal of Geophysical Research: Earth Surface* 116(F1): F01013,.DOI 10.1029/2010JF001931.

Li B, Roberts RG and Jacobs Z, 2013. On the dose dependency of the bleachable and non-bleachable components of IRSL from K-feldspar: improved procedures for the dating of Quaternary sediments. *Quaternary Geochronology* 17: 1–13, DOI 10.1016/j.quageo.2013.03.006.

Li SH, Chen YY, Li B, Sun JM and Yang LR, 2007b. OSL dating of sediments from desert in northern China. *Quaternary Geochronology* 2(1–4): 23–28, DOI 10.1016/j.quageo.2006.05.034.

Li SH and Tso MYW, 1997. Lifetime determination of OSL signals from potassium feldspar. *Radiation Measurements* 27(2): 119–121, DOI 10.1016/S1350-4487(96)00145-X.

Li SH, Tso MYW and Wong NWL, 1997. Parameters of OSL traps determined with various linear heating rates. *Radiation*

Measurements 27(1): 43–47, DOI 10.1016/S1350-4487(96)00137-0.

Lowick SE, Trauerstein M and Preusser F, 2012. Testing the application of post IR-IRSL dating to fine grain waterlain sediments. *Quaternary Geochronology* 8: 33–40, DOI 10.1016/j.quageo.2011.12.003.

Morthekai P, Jain M, Murray AS, Thomsen KJ and Bøtter-Jensen L, 2008. Fading characteristics of martian analogue materials and the applicability of a correction procedure. *Radiation Measurements* 43(2–6): 672–678, DOI 10.1016/j.radmeas.2008.02.019.

Murray AS, Buylaert JP, Thomsen KJ and Jain M, 2009. The effect of preheating on the IRSL signal from feldspar. *Radiation Measurements* 44(5–6): 554–559, DOI 10.1016/j.radmeas.2009.02.004.

Murray AS and Roberts RG, 1998. Measurement of the equivalent dose in quartz using a regenerative-dose single-aliquot protocol. *Radiation Measurements* 29(5): 503–515, DOI 10.1016/S1350-4487(98)00044-4.

Murray AS, Thomsen KJ, Masuda N, Buylaert JP and Jain M, 2012. Identifying well-bleached quartz using the different bleaching rates of quartz and feldspar luminescence signals. *Radiation Measurements* 47(9): 688–695, DOI 10.1016/j.radmeas.2012.05.006.

Murray AS and Wintle AG, 2000. Luminescence dating of quartz using an improved single-aliquot regenerative-dose protocol. *Radiation Measurements* 32(1): 57–73, DOI 10.1016/S1350-4487(99)00253-X.

Poolton NRJ, Kars RH, Wallinga J and Bos AJJ, 2009. Direct evidence for the participation of band-tails and excited-state tunnelling in the luminescence of irradiated feldspars. *Journal of Physics: Condensed Matter* 21: 485505, DOI 10.1088/0953-8984/21/48/485505.

Poolton NRJ, Ozanyan KB, Wallinga J, Murray AS and Bøtter-Jensen L, 2002. Electrons in feldspar II: a consideration of the influence of conduction band-tail states on luminescence processes. *Physics and Chemistry of Minerals* 29(3): 217–225, DOI 10.1007/s00269-001-0218-2.

Qin JT and Zhou LP, 2012. Effects of thermally transferred signals in the post-IR IRSL SAR protocol. *Radiation Measurements* 47(9): 710–715, DOI 10.1016/j.radmeas.2011.12.011.

Ramos AM, Cunha PP, Cunha LS, Gomes A, Lopes FC, Buylaert JP and Murray AS, 2012. The River Mondego terraces at the Figueira da Foz coastal area (western central Portugal): Geomorphological and sedimentological characterization of a terrace staircase affected by differential uplift and glacio-eustasy. *Geomorphology* 165–166: 107–123, DOI 10.1016/j.geomorph.2012.03.037.

Reimann T and Tsukamoto S, 2012. Dating the recent past (<500 years) by post-IR IRSL feldspar - Examples from the North Sea and Baltic Sea coast. *Quaternary Geochronology* 10: 180–187, DOI 10.1016/j.quageo.2012.04.011.

Reimann T, Tsukamoto S, Naumann M and Frechen M, 2011. The potential of using K-rich feldspars for optical dating of young coastal sediments - A test case from Darss-Zingst peninsula (southern Baltic Sea coast). *Quaternary Geochronology* 6(2): 207–222, DOI 10.1016/j.quageo.2010.10.001.

Roberts HM, 2012. Testing Post-IR IRSL protocols for minimising fading in feldspars, using Alaskan loess with independent chronological control. *Radiation Measurements* 47(9): 716–724, DOI 10.1016/j.radmeas.2012.03.022.

Roberts RG, Galbraith RF, Olley JM, Yoshida H and Laslett GM, 1999. Optical dating of single and multiple grains of quartz from jinmium rock shelter, northern Australia, part 2, Results and implications. *Archaeometry* 41(2): 365–395, DOI 10.1111/j.1475-4754.1999.tb00988.x.

Roskosch J, Tsukamoto S, Meinsen J, Frechen M and Winsemann J, 2012. Luminescence dating of an Upper Pleistocene alluvial fan and aeolian sandsheet complex: The Senne in the Munsterland Embayment, NW Germany. *Quaternary Geochronology* 10: 94–101, DOI 10.1016/j.quageo.2012.02.012.

Sanderson DCW and Clark RJ, 1994. Pulsed photostimulated luminescence of alkali feldspars. *Radiation Measurements* 23(2–3): 633–639, DOI 10.1016/1350-4487(94)90112-0.

Schatz AK, Buylaert JP, Murray A, Stevens T and Scholten T, 2012. Establishing a luminescence chronology for a palaeosol-loess profile at Tokaj (Hungary): A comparison of quartz OSL and polymineral IRSL signals. *Quaternary Geochronology* 10: 68–74, DOI 10.1016/j.quageo.2012.02.018.

Schmidt ED, Frechen M, Murray AS, Tsukamoto S and Bittmann F, 2011. Luminescence chronology of the loess record from the Tonchesberg section: A comparison of using quartz and feldspar as dosimeter to extend the age range beyond the Eemian. *Quaternary International* 234(1–2): 10–22, DOI 10.1016/j.quaint.2010.07.012.

Sohbati R, Murray AS, Buylaert JP, Ortuno M, Cunha PP and Masana E, 2012. Luminescence dating of Pleistocene alluvial sediments affected by the Alhama de Murcia fault (eastern Betics, Spain) - a comparison between OSL, IRSL and post-IR IRSL ages. *Boreas* 41(2): 250–262, DOI 10.1111/j.1502-3885.2011.00230.x.

Spooner NA, 1992. Optical Dating: Preliminary-Results on the Anomalous Fading of Luminescence from Feldspars. *Quaternary Science Reviews* 11(1–2): 139–145, DOI 10.1016/0277-3791(92)90055-D.

Spooner NA, 1994. The anomalous fading of infrared-stimulated luminescence from feldspars. *Radiation Measurements* 23(2–3): 625–632, DOI 10.1016/1350-4487(94)90111-2.

Stevens T, Markovic SB, Zech M, Hambach U and Sumegi P, 2011. Dust deposition and climate in the Carpathian Basin over an independently dated last glacial-interglacial cycle. *Quaternary Science Reviews* 30(5–6): 662–681, DOI 10.1016/j.quascirev.2010.12.011.

Templer RH, 1985. The Removal of Anomalous Fading in Zircon. *Nuclear Tracks and Radiation Measurements* 10(4–6): 531–537, DOI 10.1016/0735-245X(85)90054-7.

Thiel C, Buylaert JP, Murray A, Terhorst B, Hofer I, Tsukamoto S and Frechen M, 2011a. Luminescence dating of the Stratzing loess profile (Austria) - testing the potential of an elevated temperature post-IR IRSL protocol. *Quaternary International* 234(1–2): 23-31, DOI 10.1016/j.quaint.2010.05.018.

Thiel C, Buylaert JP, Murray AS, Elmejdoub N and Jedoui Y, 2012. A comparison of TT-OSL and post-IR IRSL dating of coastal deposits on Cap Bon peninsula, north-eastern Tunisia. *Quaternary Geochronology* 10: 209–217, DOI 10.1016/j.quageo.2012.03.010.

Thiel C, Buylaert JP, Murray AS and Tsukamoto S, 2011b. On the applicability of post-IR IRSL dating to Japanese loess. *Geochronometria* 38(4): 369–378, DOI 10.2478/s13386-011-0043-4.

Thiel C, Buylaert J-P, Murray AS, Terhorst B, Tsukamoto S, Frechen M and Sprafke T, 2011c. Investigating the chronostratigraphy of prominent palaeosols in Lower Austria using post-IR IRSL dating. *Quaternary Science Journal* 60(1): 137–152, DOI 10.3285/eg.60.1.10.

Thiel C, Terhorst B, Jaburová I, Buylaert J-P, Murray AS, Fladerer FA, Damm B, Frechen M and Ottner F, 2011d. Sedimentation and erosion processes in Middle to Late Pleistocene sequences exposed in the brickyard of Langenlois/Lower Austria. Geomorphology 135(3–4): 295–307, DOI 10.1016/j.geomorph.2011.02.011.

Thomsen KJ, Murray AS and Jain M, 2011. Stability of IRSL signals from sedimentary K-feldspar samples. *Geochronometria* 38(1): 1–13, DOI 10.2478/s13386-011-0003-z.

Thomsen KJ, Murray AS, Jain M and Botter-Jensen L, 2008. Laboratory fading rates of various luminescence signals from feldspar-rich sediment extracts. *Radiation Measurements* 43(9–10): 1474–1486, DOI 10.1016/j.radmeas.2008.06.002.

Thomsen KJ, Murray AS, Jain M and Buylaert JP, 2012. Re 'Luminescence dating of K-feldspar from sediments: a protocol without anomalous fading correction' by Bo Li and Sheng-Hua Li. *Quaternary Geochronology* 8: 46–48, DOI 10.1016/j.quageo.2011.07.002.

Tsukamoto S, Denby PM, Murray AS and Botter-Jensen L, 2006. Time-resolved luminescence from feldspars: New insight into fading.

Radiation Measurements 41(7–8): 790–795, DOI 10.1016/j.radmeas.2006.05.013.

Valladas G and Valladas H, 1979. *High temperature thermoluminescence*. Proceedings of the 18th International Symposium on Archaeometry and Archaeological Prospection, Bonn: 506–510.

Vasiliniuc S, Vandenberghe DAG, Timar-Gabor A, Panaiotu C, Cosma C and van den Haute P, 2012. Testing the potential of elevated temperature post-IR IRSL signals for dating Romanian loess. *Quaternary Geochronology* 10: 75–80, DOI 10.1016/j.quageo.2012.02.014.

Visocekas R, 1985. Tunneling radiative recombination in labradorite: its association with anomalous fading of thermoluminescence. *Nuclear Tracks and Radiation Measurements* 10(4–6): 521–529, DOI 10.1016/0735-245X(85)90053-5.

Visocekas R, Spooner NA, Zink A and Blanc P, 1994. Tunnel afterglow, fading and infrared-emission in thermoluminescence of feldspars. *Radiation Measurements* 23(2–3): 377–385, DOI 10(4–6): 521–529, DOI 10.1016/0735-245X(85)90053-5.

Wacha L and Frechen M, 2011. The geochronology of the "Gorjanovic loess section" in Vukovar, Croatia. *Quaternary International* 240(1–2): 87–99, DOI 10.1016/j.quaint.2011.04.010.

Wallinga J, Murray A and Wintle A, 2000. The single-aliquot regenerative-dose (SAR) protocol applied to coarse-grain feldspar. *Radiation Measurements* 32(5–6): 529–533, DOI 10.1016/S1350-4487(00)00091-3.

Wang XL and Wintle AG, 2013. Investigating the contribution of recuperated TL to post-IR IRSL signals in a perthitic feldspar. *Radiation Measurements* 49: 82–87, DOI 10.1016/j.radmeas.2012.12.003.

Watanuki T, Murray AS and Tsukamoto S, 2005. Quartz and polymineral luminescence dating of Japanese loess over the last 0.6 Ma: Comparison with an independent chronology. *Earth and Planetary Science Letters* 240(3–4): 774–789, DOI 10.1016/j.epsl.2005.09.027.

Wintle AG, 1973. Anomalous fading of thermoluminescence in mineral samples. *Nature* 245: 143–144, DOI 10.1038/245143a0.

Wintle AG and Murray AS, 2006. A review of quartz optically stimulated luminescence characteristics and their relevance in single-aliquot regeneration dating protocols. *Radiation Measurements* 41(4): 369–391, DOI 10.1016/j.radmeas.2005.11.001.

Zhao H and Li SH, 2002. Luminescence isochron dating: a new approach using different grain sizes. *Radiation Protection Dosimetry* 101: 333–338.